

# **Access and Binding of Local Anesthetics in the Closed Sodium Channel**

Iva Bruhova, Denis B. Tikhonov and Boris S. Zhorov

Department of Biochemistry and Biomedical Sciences, McMaster University, Hamilton, Ontario, Canada (I.B., D.B.T., B.S.Z); and Sechenov Institute of Evolutionary Physiology and Biochemistry, Russian Academy of Sciences, St. Petersburg, Russia (D.B.T.)

**Running title:** Block of the closed Na<sup>+</sup> channel

**Address correspondence to:** Boris S. Zhorov, Department of Biochemistry and Biomedical Sciences, McMaster University, Hamilton, Ontario, Canada. Tel. (905) 525-9140 x. 22049. FAX 905-522-9033. E-mail: [zhorov@mcmaster.ca](mailto:zhorov@mcmaster.ca)

Number of text pages: **26** (including Title, Running Title, and Abstract pages)

Number of tables: **2**

Number of figures: **8**

Number of references: **79**

Number of words in the Abstract: **307**

Number of words in the Introduction: **1553**

Number of words in Discussion: **2544**

**Abbreviations:** CTX, Conotoxin, DEKA, the selectivity-filter ring of Asp, Glu, Lys, and Ala residues from the four P-loop domains of Na<sup>+</sup> channels; LAs, local anesthetics; MCM, Monte Carlo-Minimization; TTX, tetrodotoxin

## ABSTRACT

Local anesthetics (LAs) are known to bind Na<sup>+</sup> channels in the closed, open, and inactivated states and reach their binding sites via extracellular and intracellular access pathways. Despite intensive studies, no atomic-scale theory is available to explain the diverse experimental data on the LA actions. Here we attempt to contribute to this theory by simulating access and binding of LAs in the KcsA-based homology model of the closed Na<sup>+</sup> channel. We used Monte Carlo minimizations to model the channel with representative local anesthetics QX-314, cocaine, and tetracaine. We found the nucleophilic central cavity to be a common binding region for the ammonium group of LAs, whose aromatic group can extend either along the pore axis (vertical binding mode) or to the III/IV domain interface (horizontal binding mode). The vertical mode was earlier predicted for the open channel, but only the horizontal mode is consistent with mutational data on the closed-channel block. To explore hypothetical access pathways of the permanently charged QX-314, we pulled the ligand via the selectivity filter, the closed activation gate, and the III/IV domain interface. Only the last pathway, which leads to the horizontal binding mode, does not impose steric obstacles. The LA ammonium group mobility within the central cavity is more restricted in the vertical mode than in the horizontal mode. Therefore, occupation of the selectivity-filter DEKA locus by a Na<sup>+</sup> ion destabilizes the vertical mode thus favoring the horizontal mode. LA binding in the closed channel requires the resident Na<sup>+</sup> ion to leave the nucleophilic central cavity through the selectivity filter, whereas the LA egress should be coupled with reoccupation of the cavity by Na<sup>+</sup>. This hypothesis on the coupled movement of Na<sup>+</sup> and LA in the closed channel explains seemingly contradictory data on how the outer-pore mutations as well as tetrodotoxin and  $\mu$ -conotoxin binding affect the ingress and egress of LAs.

## INTRODUCTION

Voltage-gated Na<sup>+</sup> channels are involved in the generation of action potentials in excitable cells. Structural determinants of major physiological characteristics, namely ion selectivity, gating, and ligand binding are localized in the  $\alpha$  subunit (Catterall, 2000; Hille, 2001). It is composed of four homologous domains (I-IV) quasi-symmetrically arranged around the central pore (Sato et al., 2001). Each domain contains six transmembrane segments (S1-S6), a pore-forming region (P), and the intracellular N- and C-ends (Denac et al., 2000; Guy and Seetharamulu, 1986). The P-region contains the selectivity filter formed by a circular motif of highly conserved D, E, K, and A residues called the DEKA locus (Heinemann et al., 1992; Terlau et al., 1991). The selectivity filter separates the outer pore, which is targeted by tetrodotoxin (TTX), saxotoxin, and conotoxins, from the inner pore, which is targeted by local anesthetics (LAs) and other small cationic drugs, see ref. (Zhorov and Tikhonov, 2004). Na<sup>+</sup> channels exist in the closed, open, fast-inactivated, and several slow-inactivated states. Structural features of the first three states are thought to be analogous to corresponding X-ray structures of K<sup>+</sup> channels (Doyle et al., 1998; Jiang et al., 2003a; Zhou et al., 2001). A structural model of the outer pore in the slow-inactivated channel has been recently proposed (Tikhonov and Zhorov, 2007).

Blockade of Na<sup>+</sup> channels by LAs is a well-known and medically important phenomenon. The mechanisms of action and structure-function relationships of LAs have been intensively studied more than 30 years (Catterall, 2000; Fozzard et al., 2005; Nau and Wang, 2004; Ruetsch et al., 2001). Inside the Na<sup>+</sup> channel pore, LAs bind state-dependently. Various LAs including etidocaine (Ragsdale et al., 1994), cocaine (Wright et al., 1998), and cocaethylene (Xu et al., 1994) block the closed Na<sup>+</sup> channel. Three terms are used to describe this phenomenon: the

closed-channel block, tonic block, or resting-channel block. In this paper we use the first term. Under high-frequency stimulation, the blocking effect increases. This phenomenon is called frequency-dependent or use-dependent block. Experiments on the state-dependent action of LAs demonstrated that generally LAs have a stronger potency in the open or inactivated channels compared to the closed channels (Chahine et al., 1992; Hille, 1977; Ragsdale et al., 1994; Wright et al., 1997; Xu et al., 1994). Two major hypotheses have been proposed to explain these effects. According to the “modulated receptor” hypothesis (Hille, 1977), LAs can bind to the closed, open and inactivated channel states, but with different affinity. According to the “guarded receptor” hypothesis (Starmer et al., 1984), LAs have a permanent affinity to their receptor, while the block depends on the frequency and duration of the channel gating, which imposes an energy barrier for the ingress and egress of the ligand.

Intensive mutational studies (Li et al., 1999; Ragsdale et al., 1994; Wright et al., 1998; Yarov-Yarovoy et al., 2001; Yarov-Yarovoy et al., 2002) demonstrated that the binding site for LAs is located in the inner pore, between the activation gate and the selectivity filter and involves residues in domains I, III, and IV. Residues in domain IV (see Methods for the residue labeling scheme), particularly F<sup>4i15</sup> and Y<sup>4i22</sup> were found critical for the use-dependent block by LAs (Ragsdale et al., 1994). Interestingly, mutations of these residues had qualitatively different effects on the closed-channel and use-dependent block. Closed-channel block by tetracaine requires a hydrophobic residue in position 4i15, while Y<sup>4i22</sup> is important for the use-dependent block (Li et al., 1999). In agreement to these results, use-dependent block by cocaine is sensitive to mutations F<sup>4i15</sup>C and Y<sup>4i22</sup>C (O'Leary and Chahine, 2002). In case of the closed-channel block by cocaine, mutation Y<sup>4i22</sup>K had no effect, whereas mutations F<sup>4i15</sup>K and N<sup>4i20</sup>K decreased the cocaine potency by 2- and 3-folds, respectively (Wright et al., 1998). In contrast, the cocaine potency in the inactivated channel decreased in the same mutants, 6-, 21.3-, and 27.4-fold,

respectively, indicating that cocaine blocks the channel state-dependently (Wright et al., 1998). The mechanisms responsible for qualitatively different effect of mutations on the closed-channel block and use-dependent block are unresolved.

The access of LAs to and from the open pore is conceptually clear. Upon channel activation, LAs enter through the open intracellular gate and move along the ion-conducting hydrophilic pathway to their binding site in the inner pore. Understanding of the hydrophilic pathway was advanced by the X-ray structures of  $K^+$  channels that have been crystallized in the closed (Doyle et al., 1998) and open states (Jiang et al., 2002a; Jiang et al., 2002b; Jiang et al., 2003a; Jiang et al., 2003b; Long et al., 2005a; Long et al., 2005b). In the open conformation, the inner helices bend and form a wide vestibule, which is readily accessible for drugs from the cytoplasm.

In the closed state, the straight inner helices converge at the cytoplasmic side and obstruct ion permeation (Doyle et al., 1998). The bulky LA molecules are unlikely to pass through the closed gate. It was suggested that LAs reach the inner pore of the closed channel via a hydrophobic pathway (Hille, 1977). Since lipid-soluble compounds can cross the membrane, they are active when applied both the extra- and intracellularly (Nettleton and Wang, 1990). Quaternary analogs of LAs such as QX-222 and QX-314 cannot cross the membrane and therefore are used as probes for exploring the access pathways into the channels. When applied intracellularly, the quaternary LAs can only block the open  $Na^+$  channels (Hille, 1977). Unlike neuronal ( $Na_v1.2$ ) and skeletal-muscle ( $Na_v1.4$ ) channels, cardiac ( $Na_v1.5$ )  $Na^+$  channels are blocked by quaternary LAs applied extracellularly (Alpert et al., 1989; Qu et al., 1995). The mutation  $F^{415}A$  of  $Na_v1.5$  effects both intra- and extracellular block by QX-314 suggesting that extracellular and intracellular LAs target the same site in the inner pore (Qu et al., 1995).

Several studies suggest that extracellularly applied LAs can reach their binding site through the outer pore. TTX binding to the outer pore of Na<sub>v</sub>1.5 reduced the external QX-314 access and recovery after the use-dependent block (Qu et al., 1995). Mutations of Na<sub>v</sub>1.4 also showed the involvement of the DEKA locus in the external access and binding of QX-314 (Sunami et al., 1997). Residue Y<sup>1p51</sup>, which is critical for isoform-specific TTX action, affects the external access of QX-222 (Sunami et al., 2000). Mutation S<sup>4p49</sup>L, one position upstream the DEKA locus, enhanced the external QX-314 access and dissociation (Sasaki et al., 2004). Cys substitutions of T<sup>3p48</sup>, F<sup>3p49</sup>, and S<sup>4p49</sup> are accessible by the externally applied Cd<sup>2+</sup> (Yamagishi et al., 1997) and sulfhydryl reagents (Struyk and Cannon, 2002; Yamagishi et al., 1997). All these data support a hypothesis that the outer pore of Na<sup>+</sup> channels may be permeable to LAs and compounds of similar size.

Another set of data suggests the involvement of the inner helices in the hydrophobic pathway of LAs. The mutation of T<sup>4i8</sup> in Na<sub>v</sub>1.5 to V, which is a native residue in Na<sub>v</sub>1.2, reduced block by external QX-314 (Qu et al., 1995). Mutation of I<sup>4i11</sup>A created an external pathway for LAs in the brain (Ragsdale et al., 1994) and muscle Na<sup>+</sup> channels (Sunami et al., 2001; Wang et al., 1998). This mutation does not affect ion permeation or binding of toxins to the outer pore (Sunami et al., 2001). A μ-CTX mutant R13N binds to the outer pore of Na<sup>+</sup> channels, but does not fully block the current. External QX-222 increased block of the I<sup>4i11</sup>A Na<sub>v</sub>1.4 mutant in the presence of the μ-CTX mutant R13N suggesting that the outer pore is not the access route for the LA (Sunami et al., 2001). Furthermore, the mutation I<sup>4i11</sup>C in Na<sub>v</sub>1.5 enhanced binding and facilitated escape of cocaethylene from the closed channel (O'Leary et al., 2003).

The coexistence of two pathways for charged LAs, one through the outer pore and another through the domain interface, was previously discussed (Lee et al., 2001). Based on the models of Na<sub>v</sub>1.4 and Na<sub>v</sub>1.5, we earlier hypothesized that the hydrophobic pathway goes through the

“sidewalk” along the IIP helix between the inner helices IIIS6 and IVS6 (Tikhonov et al., 2006; Tikhonov and Zhorov, 2005a). In this study, we elaborate this hypothesis by docking various ligands and exploring computationally various hypothetical access pathways.

In the absence of X-ray structures of voltage-gated Na<sup>+</sup> channels, their homology models have been proposed to explain the effects of LAs (Lipkind and Fozzard, 2005; Tikhonov et al., 2006; Tikhonov and Zhorov, 2007). Unlike previous studies that were focused on explaining the use-dependent block, the goal of this study is to explore access pathways and binding of LAs in the closed Na<sup>+</sup> channel. We address the following questions. What are the binding modes of QX-314, cocaine, and tetracaine in the closed channel? What are the energetically possible ingress and egress routes for LAs in the closed channel? What is the impact of Na<sup>+</sup> ions in the pore on the access and binding of LAs in the closed channel? Our study predicts that the LA molecules adopt different orientations in the closed and open channels. The energetically most favorable pathway for the LA molecule to and from the closed channel is the interface between domains III and IV, whereas the selectivity filter and the closed activation gate impose large energy barriers for LAs. Finally, we propose that the occupancy of the pore with a Na<sup>+</sup> ion affects both access and binding of LAs. These results provide a novel structural interpretation for a large body of experimental data.

## METHODS

Our model of the closed rNa<sub>v</sub>1.5 included the outer helices, P-loops, and the inner helices whose backbones were built according to the X-ray structure of KcsA (Doyle et al., 1998). Extracellular linkers between the P-loops and transmembrane helices were not modeled. The



ascending limbs of P-loops including the selectivity filter were taken from our earlier model (Tikhonov and Zhorov, 2005a). The sequences of P-loops and inner helices of  $K^+$  and  $Na^+$  channels were aligned as proposed earlier (Zhorov and Tikhonov, 2004). The outer helices, which align unambiguously between  $Na^+$  and  $Ca^{2+}$  channels, were aligned with KcsA as proposed by Huber et al. (Huber et al., 2000). Ionizable residues were treated as neutral except for the DEKA-locus ionizable residues, which were charged. The EEDD locus of the outer pore was proposed to bind four  $Na^+$  ions between domains (Tikhonov and Zhorov, 2007). To make the locus more flexible, we did not use here the interdomain  $Na^+$  bridges but neutralized the four acidic residues by four protons. Since the EEDD locus is more than 15 Å away from the binding site of LAs in the inner pore, this approximation would bias the LAs access through the selectivity filter, but is unlikely to affect the ligand binding in the inner pore. Cocaine and tetracaine models were protonated based on the data that protonated cocaine blocks  $Na^+$  channels (Nettleton and Wang, 1990). The DEKA locus was loaded either by an explicit water molecule or a  $Na^+$  ion, which were initially constrained, respectively to the D and K or D and E side chains. In the subsequent MCM trajectories the constraints were removed, but neither the water molecule nor the  $Na^+$  ion moved away from the DEKA locus.

A universal scheme (Zhorov and Tikhonov, 2004) was used for residue labeling (Table 1). It includes the domain number (1-4), symbols “i”, “p”, or “o” for the inner helix, P-loop, or the outer helix, and the relative number from the N-end of a transmembrane helix or from the DEKA-locus positions *1p50*, *2p50*, etc. For example,  $M^{2i11}$  designates methionine in the domain II inner helix, 11 positions downstream from its N-end.

The Monte Carlo-energy minimization (MCM) method (Li and Scheraga, 1987) was used to search for energetically favourable conformations in the space of torsional angles, bond angles of ligands, and positions and orientations of root atoms of free molecules. Alpha carbons were

constrained to the template structure by pins. A pin is a flat-bottom energy function that allows atoms to deviate penalty-free up to 1 Å from the template and imposes a penalty of 10 kcal mol<sup>-1</sup> Å<sup>-1</sup> for larger deviations.

The atomic charges of ligands were calculated by the AM1 method (Dewar et al., 1985) using the MOPAC program. Hydration energy was calculated by the implicit-solvent method (Lazaridis and Karplus, 1999). Hydration of the lipid-facing residues in the outer helices is unrealistic, but because these residues are not involved in the binding of LAs and because the channel folding does not change in our model, the hydration of S5s has a minimal impact on our results.

Nonbonded interactions were calculated using the AMBER force field (Weiner et al., 1984; Weiner et al., 1986). The ligands contained both heavy atoms and hydrogens. The protein was modeled in the united-atom approximation, but an all-atom model was also used to assess cation- $\pi$  interactions of the ligand with aromatic residues. A cutoff of 8 Å was used for nonbonded interactions, but those involving ions and ionized groups were calculated without a cutoff. The homology model of the ligand-free closed channel was MC-minimized until 2,000 consecutive energy minimizations did not decrease the energy of the apparent global minimum found. For docking of LAs, the multi-MCM protocol (Bruhova and Zhorov, 2007; Tikhonov and Zhorov, 2007) was employed as follows. First, 60,000 starting points with random positions, orientations, and conformations of the ligand were seeded within a 14 Å-edge cube whose center was placed in the cavity center. The size of the cube was chosen to ensure sampling in the central pore and in the domain interfaces. Each starting point was optimized in an MCM trajectory of 10 steps to remove steric overlaps with the channel. Three hundreds lowest-energy structures found at this stage were further MC-minimized in longer trajectories to refine the protein-ligand

complexes. These trajectories were terminated after 1,000 consecutive steps did not decrease the energy. All the complexes within 10 kcal/mol from the apparent global minimum were analyzed.

Access pathways for LAs were explored by pulling QX-314 along a specific direction with the step of 0.5 Å (Tikhonov and Zhorov, 1998). At each position, the energy was MC-minimized. For QX-314 pulled through the selectivity filter or the closed activation gate, the pulling direction coincides with the pore axis. For the ligand pulled between domains III and IV, the pulling direction is parallel to helix IIP. The ligand was pulled by the *para*-carbon of the benzene ring. The ligand flip-flop was prevented as described (Bruhova and Zhorov, 2007). For each pathway, three independent trajectories were calculated and the ligand-channel energies at each position were averaged. All calculations were performed using the ZMM program ([www.zmmsoft.com](http://www.zmmsoft.com)).

## RESULTS

### *LA Binding*

Three structurally different LAs were chosen in our study: QX-314, which is a permanently charged derivative of lidocaine, cocaine with bulky fused rings, and tetracaine with an elongated hydrophobic tail attached to its benzene ring (Fig. 1). The LAs were docked in the closed Na<sub>v</sub>1.5 model whose DEKA locus was loaded by either a water molecule (H<sub>2</sub>O-DEKA model) or a Na<sup>+</sup> ion (Na<sup>+</sup>-DEKA model).

*LAs in the H<sub>2</sub>O-DEKA model.* Figures 2A,B show multiple randomly generated starting points. The multi-MCM of the starting points yielded ensembles of 50 most favorable complexes for each of the three compounds studied. In each complex, the ligand occurred in the inner pore. In most cases, the ammonium group was found in the central cavity, near the focus of P-helices

(Figs. 2C, 3A). The DEKA-locus side chains strongly contribute to the binding of all three LAs because the electrostatic attraction of the ammonium group to D<sup>1p50</sup> and E<sup>2p50</sup> outweighs the repulsion from K<sup>3p50</sup>. Furthermore, carbonyl groups of residues in positions *p47* through *p50* of all four repeats also stabilize the ligand via electrostatic interactions.

The ligand orientation greatly varied between the complexes. All three LAs have an elongated shape. Let us define the long axis of a ligand as a line drawn between the ammonium nitrogen and the *para*-carbon of the benzene ring. Three energetically favorable binding modes of LAs inside the channel can be categorized as vertical, horizontal, and angular. In the first two modes, the ligand long axis is either parallel or perpendicular to the pore axis (Fig. 2 D,F). In the angular mode, the ligand long axis is at 45±10° to the pore axis (Fig. 2 E). QX-314 (Fig. 2) and cocaine (Fig. 3) can adopt all the three binding modes. Tetracaine (Fig. 4) adopts only the horizontal mode because its long hydrophobic tail does not fit in the closed pore.

Energetics of the binding modes is given in Table 2. The vertical mode is stabilized by rings of residues in positions *i22* and *i15*. In the vertical mode, the hydrophobic bundle of residues *i22* from all four repeats anchors the LA benzene ring (Figs. 2D and 3C). In particular, F<sup>2i22</sup> and Y<sup>4i22</sup>  $\pi$ -stack to opposite faces of the drug's benzene ring. In some cases the ligand's carbonyl or the secondary amine group H-bonds with the OH group of Y<sup>4i22</sup>. Residue F<sup>3i22</sup> at the bottom of the binding pocket interacts with the benzene ring in the edge-to-face manner (Burley and Petsko, 1985; Singh and Thornton, 1985). I<sup>1i22</sup> also contributes to the bottom of the binding pocket, while F<sup>4i15</sup> binds to the ligand side.

In the horizontal binding mode the aromatic ring protrudes in the III/IV domain interface. Despite this orientation was not biased in our calculations, practically no low-energy complexes were found in which the aromatic ring of LAs were protruding in the other (I/II, II/III, or IV/I) domain interfaces. Only in the case of tetracaine, a few complexes were found where the

aromatic ring protruded in the other interfaces, but their ligand-channel energy was weak. The horizontal binding mode is stabilized mainly by  $\pi$ -stacking interactions with F<sup>4i15</sup> (Table 2). Due to the horizontal ligand orientation, residues in the cytoplasmic halves of S6s practically do not contribute to the ligand binding. The long tail of tetracaine reaches W<sup>3o18</sup> that contributes -0.7 kcal/mol to ligand-channel energy. In the angular binding mode, which is intermediate between the vertical and horizontal modes, the benzene ring of the ligands binds between F<sup>4i15</sup> and Y<sup>4i22</sup>.

Generally, the horizontal binding mode has more preferable electrostatic energy than the vertical one due to a stronger attraction of the ligand's ammonium group to the nucleophilic C-ends of the P-helices (Table 2). This is compensated by a larger dehydration cost of the horizontal mode *vs.* the vertical one. Interactions with the S6s are more important for the vertical mode. Contributions of the key binding determinants in IVS6 to the vertical and horizontal modes are different: in the vertical mode, Y<sup>4i22</sup> contributes more than F<sup>4i15</sup>, but only F<sup>4i15</sup> contributes significantly to the horizontal mode. The above characteristics of the binding modes are similar for the three LA docked in this study suggesting that other LAs may bind similarly in the closed Na<sup>+</sup> channel.

*LAs in the Na<sup>+</sup>-DEKA model.* Earlier we predicted that the binding mode of lidocaine in the open Na<sup>+</sup> channel depends dramatically on whether a Na<sup>+</sup> ion or a water molecule populates the DEKA locus (Tikhonov et al., 2006; Tikhonov and Zhorov, 2007). In this study, we placed a Na<sup>+</sup> ion in outer pore of the closed Na<sub>v</sub>1.5 in a position equivalent to the K<sup>+</sup> ion position 4 in the outer pore of K<sup>+</sup> channels (Tikhonov and Zhorov, 2007). In this position, the Na<sup>+</sup> ion counterbalances the excessive negative charge in the DEKA locus, which becomes less attractive for the pore-bound cations than in the H<sub>2</sub>O-DEKA model.

Cocaine and QX-314 were docked by the multi-MCM method. In the majority of the 50 lowest-energy structures collected for each ligand, the ammonium group is displaced from the

selectivity filter in the cytoplasmic direction due to electrostatic repulsion from the Na<sup>+</sup> ion in the DEKA locus. In the vertical binding mode, the repulsion energy between the ammonium group and the Na<sup>+</sup> ion is as strong as 13.0 kcal/mol. Because of the limited space in the central cavity, the drugs had a tendency to adopt the horizontal binding mode with the aromatic ring protruding in the III/IV domain interface (Fig. 3 B). In this mode, the ligand ammonium group and the Na<sup>+</sup> ion are more distant from each other than in the vertical mode. As a consequence, the repulsion between the Na<sup>+</sup> ion and the ligand in the horizontal binding mode varies from 1.5 to 8 kcal/mol, which is much weaker than in the vertical mode (Table 2). In the lowest-energy complex, the cocaine ester group is attracted by the Na<sup>+</sup> ion, while the benzene ring  $\pi$ -stacks with F<sup>415</sup> (Fig. 3 D). In some complexes, the Na<sup>+</sup> ion relocated from the starting position to the extracellular face of the DEKA locus (Fig. 3 D), the level equivalent to position 2 in K<sup>+</sup> channels (Tikhonov and Zhorov, 2007). This relocation decreased the Na<sup>+</sup>-ligand repulsion.

Thus, in the Na<sup>+</sup>-DEKA and H<sub>2</sub>O-DEKA models the LAs adopt the horizontal and vertical binding modes, respectively and the LA binding energy significantly depends on the occupancy of the DEKA locus.

The above docking experiments of our study have been performed with the united-atom model of the channel, which is insensitive to cation- $\pi$  interactions because atomic charges at aromatic carbons are close to zero. To assess a possibility of cation- $\pi$  interactions, we created and MC-minimized an all-atom model of the closed channel and docked QX-314 in the vertical and horizontal modes with constraints imposing either  $\pi$ -stacking or cation- $\pi$  interactions between QX-314 and F<sup>415</sup>. After MC-minimizing the complexes, constraints were removed and the second round of MC-minimizations provided structures shown in Fig. S1 in Supplemental Data. The structures with cation- $\pi$  interactions were found less preferable than those with stacking interactions (Table S1 in Supplemental Data).

## Access pathways of QX-314

The extracellular access of LAs to the closed Na<sup>+</sup> channels is discussed in several studies (Qu et al., 1995; Ragsdale et al., 1994; Sunami et al., 1997; Sunami et al., 2001), but it remains unclear whether LAs pass between the III/IV domain interface or through the selectivity filter. To address this, we pulled QX-314 through these two hypothetical pathways (Figs. 5, 6). As a control, the ligand was also pulled through the closed activation gate (Fig. 5A). The vertical binding mode was chosen as a starting position for pulling QX-314 through the selectivity filter and the closed gate, while the horizontal mode was used as the starting point for pulling the ligand via the III/IV interface. None of the computed profiles have ligand-receptor energy better than in the starting point (Figs. 5C, 7). This agrees with the notion that the inner pore is the energetically preferable binding site for LAs.

Pulling QX-314 through the closed gate (Fig. 5A) imposes a van der Waals energy barrier of 60 kcal/mol (Fig. 5C) indicating that the closed gate is impassible. Two peaks of the energy profile at positions -10 and -17 Å are determined by repulsion between the ligand's ammonium group and residues in positions *i22* and *i26*, which face the pore axis. Thus, as expected, the closed activated gate does not allow QX-314 to reach the central cavity from the cytoplasm.

Pulling QX-314 through the selectivity filter not loaded with a water molecule or a Na<sup>+</sup> ion (Fig. 5B) results in the energy barrier of 33 kcal/mol, which is caused by steric clashes and unfavorable desolvation (Fig. 5C). Residues in positions *p49* and *p50* form the tightest rings. In particular, K<sup>3p50</sup>, G<sup>2p49</sup>, and S<sup>4p49</sup> contribute to the large energy barrier. Residues in positions *p51*, *p52*, and *p53* do not impose energy barriers but attract the ligand.

Pulling QX-314 through the III/IV domain interface (Fig. 6) did not cause high-energy barriers (Fig. 7). Residues of the IIIP-helix interact with the ligand all along the pathway. The

ligand-channel energy weakens as the ligand leaves the central cavity and loses electrostatic attractions from the DEKA locus and nucleophilic C-ends of P-helices. Residues T<sup>4i8</sup> and I<sup>4i11</sup> contribute only weakly to the drug-channel energy at the drug-binding site (position 0), but their contributions increase along the pathway. The most significant interaction of QX-314 with I<sup>4i11</sup> corresponds to the rightmost part of the profile, indicating that I<sup>4i11</sup> affects the drug access much stronger than the drug binding in the inner pore. Residue T<sup>4i8</sup>, which is far from the pore axis, faces the III/IV interface. The experimentally observed effect of mutations in this position on the external drug access can be explained by direct interaction with the ligand entering the domain interface. It should be noted that both T<sup>4i8</sup> and I<sup>4i11</sup> interact with the drug at the rightmost part of the pathway (Fig. 7) and concertedly attract the ligand at this part where the ligand-channel attraction energy is rather small, while the desolvation cost increases. Therefore changes in the size and hydrophobicity in positions *4i8* and *4i11* can significantly affect access of ligands through the domain interface. Thus, the computed energy profile through the III/IV domain interface agrees with the hydrophobic access pathway concept.

Comparison of the energy profiles calculated in the H<sub>2</sub>O-DEKA and Na<sup>+</sup>-DEKA models show that the Na<sup>+</sup> ion significantly destabilizes QX-314 in position 0 and along the access pathway (Fig. 7 B). In position 0, the difference between the drug-channel energies of the two models is 5 kcal/mol. The difference in positions 3 to 6 is much larger because in this narrow part of the pathway the Na<sup>+</sup> ion and the ligand's ammonium nitrogen approach each other as close as 6 Å. Besides this electrostatic repulsion, the Na<sup>+</sup> ion does not significantly affect the ligand trajectory and contributions of individual residues to the ligand-channel energy.

Residue F<sup>4i15</sup> plays a key role in the access pathway of QX-314 (Figs. 6 and 7D). At position 0, F<sup>4i15</sup> faces the pore and  $\pi$ -stacks with the benzene ring of QX-314. As QX-314 is pulled between domains III and IV, F<sup>4i15</sup> reorients to let QX-314 pass. The reorientation causes



an energy barrier at position 3.5 Å from the start. The barrier is much higher in the Na<sup>+</sup>-DEKA model than in the H<sub>2</sub>O-DEKA model.

## DISCUSSION

Understanding molecular determinants of state-dependent action of LAs, which are widely used clinically and in experiments, are of obvious importance. Residues F<sup>4i15</sup> and Y<sup>4i22</sup> have long been known as critical determinants of the use-dependent block. LAs in the vertical but not in horizontal mode can simultaneously bind to both F<sup>4i15</sup> and Y<sup>4i22</sup>, which are separated by two helical turns of IVS6. Several structural models of Na<sup>+</sup> channels visualized the vertical binding mode and analyzed contacts of LAs with LA-sensing residues (Fozzard et al., 2005; Lipkind and Fozzard, 2000; Lipkind and Fozzard, 2005; McNulty et al., 2007; Tikhonov et al., 2006; Tikhonov and Zhorov, 2007).

It is well known that effects of mutations on the block of the open/inactivated and closed channels are different (Chahine et al., 1992; Hille, 1977; Nau et al., 2003; Ragsdale et al., 1994; Wright et al., 1997; Xu et al., 1994), but molecular determinants of this difference were unclear. Here we systematically simulated binding of structurally different LAs in the closed-channel model. The chosen LAs contain an ammonium group and a benzene ring but essentially vary in size and chemical structure. Since the central cavity in the closed channel is rather small, it was unclear how these ligands interact with ligand-sensing residues. Furthermore, since occupation of the DEKA locus in the closed state is unknown, we populated the locus by either a water molecule or a Na<sup>+</sup> ion. Unbiased docking using a powerful multi-MCM search resulted in ensembles of complexes in which QX-314 and cocaine adopted vertical, horizontal, or intermediate (angular) binding modes. In contrast, only the horizontal binding mode was found

for tetracaine, because the vertical mode of this elongated drug does not fit in the confined central cavity of the closed channel. The horizontal binding mode of tetracaine was also recently proposed by another group (Scheib et al., 2006).

Ragsdale and coauthors (Li et al., 1999) systematically studied state-dependent action of tetracaine on Na<sub>v</sub>1.3 and its mutants and demonstrated that frequency-dependent block requires an aromatic residue (F, Y, or W) in position *4i15*, while the closed-channel block requires a hydrophobic residue in this position. Furthermore, the frequency-dependent block required Y<sup>4i22</sup>, while the resting-channel block was possible with S, A, C, I, or F in this position. These data support our conclusion that tetracaine blocks the closed channel in the horizontal mode. Indeed, F<sup>4i15</sup> contributes  $-2.1$  kcal/mol, while Y<sup>4i22</sup> did not have a noticeable contribution (Table 2).

Docking of QX-314 and cocaine did not predict a single binding mode. However, experimental data suggests that the horizontal binding mode in the closed channel is preferable for these drugs and possibly other LAs. Indeed, mutation Y<sup>4i22</sup>K had no effect on the closed-channel block of rNa<sub>v</sub>1.4 by cocaine, while mutations F<sup>4i15</sup>K lowered the LA affinity twofold (Wright et al., 1998). The hNa<sub>v</sub>1.5 mutation I<sup>4i11</sup>C weakly affects the use-dependent block by cocaine, while Y<sup>4i22</sup>C had the strongest effects (O'Leary and Chahine, 2002). Thus, residues in the C-terminal half of IVS6 affect predominantly the use-dependent block, while residues at the N-terminal half affect mainly the closed-channel block. Mutation N<sup>4i20</sup>K also decreased cocaine binding threefold (Wright et al., 1998), but this residue does not face the pore in our model and probably affects the ligand binding allosterically. Indeed, mutations of N<sup>4i20</sup> affect slow inactivation (Chen et al., 2006). Thus, experimental data support the notion that LAs bind to the closed channel in the horizontal mode, but they block the open channel in the vertical mode.

A recent study (Ahern et al., 2008) provides additional support for our model. The authors used a series of fluorinated derivatives of aromatic amino acids (Santarelli et al., 2007a;

Santarelli et al., 2007b) to systematically reduce the negative electrostatic potential at aromatic carbons of F<sup>4i15</sup> and Y<sup>4i22</sup>. The disruption of pi-cation interaction of F<sup>4i15</sup> abolished the use-dependent block by lidocaine without affecting the closed-channel block. Fluorination of Y<sup>4i22</sup> had no effect. This result strongly suggests that pi-cation interactions takes place only at F<sup>4i15</sup> and only in the use-dependent block. In our models of the use-dependent block (Tikhonov et al., 2006; Tikhonov and Zhorov, 2007) the amino-groups of LAs are located near the F<sup>4i15</sup> and can form the pi-cation contact. Contrary to this, in the horizontal binding mode (that we suggest to correspond to the closed channel block) F<sup>4i15</sup> interacts with the LAs' aromatic rings rather than with the ammonium groups. Thus, despite the united-atom approximation, which is used in our model, is unable to reveal the pi-cation interactions, our models agree with experimental data (Ahern et al., 2008).

The vertical binding mode, which likely corresponds to the use-dependent block, and the horizontal binding mode, which is proposed here for the closed-channel block have similar structural components. In both binding modes, the amino-group of LAs is located below the selectivity filter in the region, which is attractive for cationic particles due to the cooperative effect of the P-helices macrodipoles. However, in the horizontal mode the aromatic moiety of the drugs faces the domain interface and the channel lumen is not completely occluded especially by ligands with a small ammonium group (lidocaine). This raises a question about the mechanism of channel block. A recent study (McNulty et al., 2007) suggested that for asymmetrically bound LAs the block is caused by a combination of electrostatic and hydrophobic effects. This mechanism is plausible and fully agrees with our models. Moreover, effects of charge and hydrophobicity on the action of sodium channel ligands were the subjects of our recent studies (Tikhonov and Zhorov, 2005b; Wang et al., 2006; Wang et al., 2007a; Wang et al., 2007b). Sodium channel activators like batrachotoxin and veratridine bind in the sodium channel to the

site, which significantly overlaps with the LA binding site. These drugs do not completely occlude the channel. The charged groups of these drugs do not face the pore. Rather, the drugs expose hydrophilic groups to the remaining lumen. As a result, the channel is conducting despite the presence of relatively large molecules in the pore. Introduction of positively charged residues in position *2i15* does not abolish channel conductance but inverses batrachotoxin action from activation to block.

### ***LA access through the III/IV domain interface***

Previous studies proposed two possible access pathways of LAs to the inner pore of the closed Na<sup>+</sup> channel: through the selectivity filter and through the domain interface (see Introduction). Residues, which when mutated affect the LA access, face either the pore axis or the domain interface (Table 1). Except for residues at the P-loop turn, which can face both pathways, all other positions face either the first or the second pathway. Both pathways were proposed to coexist (Lee et al., 2001). However, positive values of van der Waals energy at positions 10 to 13 of the pathway through the selectivity filter (Fig. 5C) indicate steric clashes of the LA molecule with the P-loop residues, which face the pore axis. In contrast, van der Waals energy component is negative all along the access pathway through the sidewalk (Fig. 7A). The existence of this pathway readily explains mutational data about the involvement of residues in positions *4i8*, *4i11*, *4i15*, and *4p49* in the extracellular access (Table 1). All these residues face the sidewalk and interact with QX-314 according to the energy profiles (Fig. 7 C, D). In particular, the Na<sub>v</sub>1.5 mutation T<sup>4i8</sup>V, which increases the sidewalk hydrophobicity, renders the channel less sensitive to the extracellular block by LAs (Qu et al., 1995). Mutation I<sup>4i11</sup>A in the muscle and brain Na<sup>+</sup> channels makes them sensitive to extracellularly applied quaternary LAs (Ragsdale et al., 1994; Sunami et al., 2001; Wang et al., 1998). Furthermore, mutation I<sup>4i11</sup>C

facilitates escape of the trapped cocaethylene from  $\text{Na}_v1.5$  (O'Leary et al., 2003). Our models explain the effects of these mutations: the bulky  $\text{I}^{4i11}$  in the wild type  $\text{Na}_v1.4$  prevents LAs to enter the pore, while smaller  $\text{A}^{4i11}$  enables LAs to pass. A naturally occurring  $\text{hNa}_v1.5$  mutation  $\text{S}^{4p49}\text{L}$  accelerates recovery from the block by internally applied QX-314, enhances the closed-channel block by mexiletine and QX-314, and attenuates the use-dependent block by mexiletine (Sasaki et al., 2004). The  $\text{S}^{4p49}\text{L}$  mutation was suggested to effect the LA access through the selectivity filter (Sasaki et al., 2004), but in our model  $\text{S}^{4p49}$  faces the sidewalk and contributes to LA binding.

The extracellular access of drugs is not an exclusive feature of  $\text{Na}^+$  channels. Mutations of various residues that face the III/IV domain interface affect binding of drugs to L-type  $\text{Ca}^{2+}$  channel (Hockerman et al., 1997). Permanently charged benzothiazepines (Hering et al., 1993; Kurokawa et al., 1997; Seydl et al., 1993) and dihydropyridines (Kass et al., 1991; Kwan et al., 1995) block the L-type  $\text{Ca}^{2+}$  channel from the extracellular side. Dihydropyridines were proposed to access  $\text{Ca}^{2+}$  channels via the III/IV domain interface (Yamaguchi et al., 2003). The recent X-ray structures of KcsA with hydrophobic cations show long hydrophobic moieties bound in the interface between S6, S5, and P-helices, which is suggested to provide an alternative access pathway for drugs to the inner pore (Lenaeus and Gross, 2008).

Our present model predicts that LAs also access the closed  $\text{Na}^+$  channel via III/IV domain interface. However, since mutations of the outer-pore residues and toxin binding in the outer pore are also known to influence the LA access into the closed channel, the challenge is to explain these experimental observations in view of our model. We propose here that the above influence is mediated by  $\text{Na}^+$  ions that can occupy two nucleophilic sites, one in the DEKA locus and another in the cavity center. The antagonism between the  $\text{Na}^+$  ion in the DEKA locus and LA binding in the open channel was described before (Tikhonov and Zhorov, 2007). Our present

calculations show that occupation of the DEKA locus by a  $\text{Na}^+$  ion also affects LA binding in the closed channel (Table 2) and hinders the LAs access to the pore via the III/IV domain interface (Fig. 7 B). In view of these data, mutations in the ascending limbs, which are likely to affect  $\text{Na}^+$  binding in the DEKA locus, should affect access of LAs through the domain interface. For example, mutations  $\text{D}^{1\text{p}50}\text{A}$  and  $\text{E}^{2\text{p}50}\text{A}$  at the DEKA locus make the  $\text{Na}_v1.4$  channel sensitive to the external QX-222 (Sunami et al., 1997). The authors of this study proposed a straightforward interpretation of the experiments, according to which substitutions of large residues in the outer pore with small residues can provide a path for the external QX-222. We do not rule out this interpretation, but in view of our calculations, the above mutations would destabilize  $\text{Na}^+$  in the DEKA locus and hence facilitate the LAs access through the domain interface.

In the X-ray structure of Kv1.2 the voltage-sensor domain does not block the sidewalk, but to enter it a ligand should interact with lipids and/or an auxiliary subunit of the channel. In the absence of experimental data, we cannot consider structural details of these interactions. A weakly hydrated tetraalkylammonium cation like QX-314 has more chances to pass by hydrophobic residues of the sidewalk than strongly hydrated inorganic or ammonium cations. For example, energy calculations suggest that trialkylammonium-methanethiosulfonate reagents, which are used in the substituted cysteine-accessibility method, can reach those levels in the pore of ion channels, which are closed for hydrated inorganic ions (Tikhonov et al., 2004; Tikhonov and Zhorov, 2007).

The facts that TTX reduces the rates of extracellular QX-314 block and recovery from the use-dependent block support a hypothesis that LA access their binding site through the selectivity-filter (Qu et al., 1995). Here we propose an alternative explanation for these observations. It involves a  $\text{Na}^+$  ion in the central cavity (Fig. 8) at position, which is equivalent to the  $\text{K}^+$  binding site seen in X-ray structures of  $\text{K}^+$  channels. Since a  $\text{Na}^+$  ion and LAs are obvious

competitors for the nucleophilic cavity center, the  $\text{Na}^+$  ion should leave this site to allow LA binding (Fig. 8A). However, the closed channel, which is blocked by TTX, does not provide the escape route for the  $\text{Na}^+$  ion. Residing the cavity, the  $\text{Na}^+$  ion prevents QX-314 access in the TTX-blocked closed channel (Fig. 8B). The TTX-induced reduction of the channel recovery from the use-dependent block can be also explained. In the absence of TTX, the escape of LAs through the sidewalk releases the nucleophilic site in the cavity center and this site will be occupied by the incoming  $\text{Na}^+$  ion. In the TTX-blocked closed channel,  $\text{Na}^+$  cannot access the cavity and replace the LA molecule. It would be an energetically non-preferable situation if a LA molecule leaves the nucleophilic cavity center and this region is not reoccupied by a  $\text{Na}^+$  ion.

In contrast to TTX, the  $\mu$ -CTX mutant R13N binds to the outer pore of  $\text{Na}^+$  channels without completely blocking the  $\text{Na}^+$  current (Sunami et al., 2001). In the  $\text{Na}_v1.4$  mutant  $\text{I}^{411}\text{A}$ , externally applied QX-222 reaches the inner pore of the toxin-bound channel and further blocks the current. In view of our model, the incomplete block of the closed channel by the peptide toxin does not prevent exchange of  $\text{Na}^+$  and LAs in the central cavity (Fig. 8C). Thus, comparison of the effects of TTX and the  $\mu$ -CTX mutant on the LA ingress and egress in the closed channel suggests that movement of inorganic and organic cations is coupled in the  $\text{Na}^+$  channel.

The residues whose mutations affect access of LAs in the closed channel are clustered in two groups: one group is localized at the sidewalk and another in the outer pore including the selectivity filter. The hypothesis of the coupled movement of organic and inorganic ions explains why mutations in both clusters affect the drug access through the sidewalk. However, it is difficult to explain how mutations of S6 residues could affect the drug access via the selectivity filter. Indeed, because the access-controlling S6 residues are not buried inside the protein, they are unlikely to allosterically affect the access via the outer pore. Furthermore, the energy profile at Fig. 7C suggests sterical hindrances for a LA molecule at the selectivity-filter level, but even in

the absence of the hindrances the coupled-movement hypothesis suggest that the access to the closed channel through the selectivity filter is unlikely. Indeed, an LA molecule approaching the central cavity through the selectivity filter would encounter an electrostatic repulsion from the  $\text{Na}^+$  ion residing in the cavity center. The  $\text{Na}^+$  ion cannot escape through the closed activation gate, or through the hydrophobic sidewalks, or through the outer pore, which is blocked by the approaching LA molecule. Therefore, displacement of the resident  $\text{Na}^+$  ion by the LA molecule coming through the selectivity filter is hardly possible.

P-loop channels have nucleophilic sites in the outer pore, the selectivity filter, and the central cavity. Numerous experimental data show that the interaction between cations at nucleophilic sites leads to the coupled movement in the multi-ion pores. For example,  $\text{K}^+$  ions are thought to move through the selectivity filter of  $\text{K}^+$  channels by sequentially occupying sites 1/3 and 2/4 (Zhou and MacKinnon, 2003). A recent experimental and theoretical study of the tetrabutylammonium-blocked KcsA shows that the position of the organic cation in the cavity depends on the selectivity-filter occupancy by  $\text{K}^+$  ions (Faraldo-Gomez et al., 2007). Here we applied the concept of the coupled movement to explain seemingly contradictory experimental data on access and binding of LAs in  $\text{Na}^+$  channels.

### ***Modeling Limitations***

In this work we used a rather simple method of energy calculations. The atom-atom energy terms included van der Waals interactions, implicit solvent, and Coulomb's electrostatics, but lacked an explicit term for cation- $\pi$  interactions. We also neglected the entropy component of free energy. Despite the limited precision of coarse-grained methods, they are widely used for homology modeling of proteins, which, like sodium channels, have a limited sequence similarity with X-ray templates. Employment of high-precision time-consuming methods in such cases



seems impractical because an assumption that the model and the template have a similar backbone geometry influences results to a greater extent than approximations of energy calculations. To compensate these limitations, we generated a large number of starting points, which cover virtually all ligand-binding scenarios (Fig. 2A,B). Subsequent MC-minimizations yielded ensembles of energetically possible binding scenarios, which include different structures (Figs. 2-4). Analysis of these ensembles allowed us to find particular binding modes, which agree with experimental data. For example, the vertical binding mode of QX-314 in the H<sub>2</sub>O-DEKA model of the closed channel corresponds to the lowest-energy structure (Table 2), but the horizontal binding mode, which has a slightly higher energy, is consistent with a large number of experimental data. Taking into account a limited precision of energy calculations in the homology model, we concluded that it is the horizontal binding mode, which correspond to the closed-channel block.

## REFERENCES

- Ahern CA, Eastwood AL, Dougherty DA and Horn R (2008) Electrostatic contributions of aromatic residues in the local anesthetic receptor of voltage-gated sodium channels. *Circ Res* **102**(1):86-94.
- Alpert LA, Fozzard HA, Hanck DA and Makielski JC (1989) Is there a second external lidocaine binding site on mammalian cardiac cells? *Am J Physiol* **257**(1 Pt 2):H79-84.
- Bruhova I and Zhorov BS (2007) Monte Carlo-energy minimization of correolide in the Kv1.3 channel: possible role of potassium ion in ligand-receptor interactions. *BMC Struct Biol* **7**:5.
- Burley SK and Petsko GA (1985) Aromatic-aromatic interaction: a mechanism of protein structure stabilization. *Science* **229**(4708):23-28.
- Catterall WA (2000) From ionic currents to molecular mechanisms: the structure and function of voltage-gated sodium channels. *Neuron* **26**(1):13-25.
- Chahine M, Chen LQ, Barchi RL, Kallen RG and Horn R (1992) Lidocaine block of human heart sodium channels expressed in *Xenopus* oocytes. *J Mol Cell Cardiol* **24**(11):1231-1236.
- Chen Y, Yu FH, Surmeier DJ, Scheuer T and Catterall WA (2006) Neuromodulation of Na<sup>+</sup> channel slow inactivation via cAMP-dependent protein kinase and protein kinase C. *Neuron* **49**(3):409-420.
- Denac H, Mevissen M and Scholtysik G (2000) Structure, function and pharmacology of voltage-gated sodium channels. *Naunyn-Schmiedeberg's Arch Pharmacol* **362**(6):453-479.
- Dewar MJS, Zoebisch EG, Healy EF and Stewart JJP (1985) AM1: A New General Purpose Quantum Mechanical Model. *J Am Chem Soc* **107**:3902-3909.

- Doyle DA, Morais Cabral J, Pfuetzner RA, Kuo A, Gulbis JM, Cohen SL, Chait BT and MacKinnon R (1998) The structure of the potassium channel: molecular basis of K<sup>+</sup> conduction and selectivity. *Science* **280**(5360):69-77.
- Faraldo-Gomez JD, Kutluay E, Jogini V, Zhao Y, Heginbotham L and Roux B (2007) Mechanism of intracellular block of the KcsA K<sup>+</sup> channel by tetrabutylammonium: insights from X-ray crystallography, electrophysiology and replica-exchange molecular dynamics simulations. *J Mol Biol* **365**(3):649-662.
- Fozzard HA, Lee PJ and Lipkind GM (2005) Mechanism of local anesthetic drug action on voltage-gated sodium channels. *Current Pharm Design* **11**(21):2671-2686.
- Guy HR and Seetharamulu P (1986) Molecular model of the action potential sodium channel. *Proc Natl Acad Sci USA* **83**(2):508-512.
- Heinemann SH, Terlau H, Stuhmer W, Imoto K and Numa S (1992) Calcium channel characteristics conferred on the sodium channel by single mutations. *Nature* **356**(6368):441-443.
- Hering S, Savchenko A, Strubing C, Lakitsch M and Striessnig J (1993) Extracellular localization of the benzothiazepine binding domain of L-type Ca<sup>2+</sup> channels. *Mol Pharmacol* **43**:820-826.
- Hille B (1977) Local anesthetics: hydrophilic and hydrophobic pathways for the drug-receptor reaction. *J Gen Physiol* **69**(4):497-515.
- Hille B (2001) *Ion channels of excitable membranes*. Sinauer Associates Inc, Sunderland, Massachusetts USA.
- Hockerman GH, Peterson BZ, Johnson BD and Catterall WA (1997) Molecular determinants of drug binding and action on L-type calcium channels. *Annu Rev Pharmacol Toxicol* **37**:361-396.

- Huber I, Wappl E, Herzog A, Mitterdorfer J, Glossmann H, Langer T and Striessnig J (2000)  
Conserved Ca<sup>2+</sup>-antagonist-binding properties and putative folding structure of a  
recombinant high-affinity dihydropyridine-binding domain. *Biochem J* **347 Pt 3**:829-836.
- Jiang Y, Lee A, Chen J, Cadene M, Chait BT and MacKinnon R (2002a) Crystal structure and  
mechanism of a calcium-gated potassium channel. *Nature* **417**(6888):515-522.
- Jiang Y, Lee A, Chen J, Cadene M, Chait BT and MacKinnon R (2002b) The open pore  
conformation of potassium channels. *Nature* **417**(6888):523-526.
- Jiang Y, Lee A, Chen J, Ruta V, Cadene M, Chait BT and MacKinnon R (2003a) X-ray structure  
of a voltage-dependent K<sup>+</sup> channel. *Nature* **423**(6935):33-41.
- Jiang Y, Ruta V, Chen J, Lee A and MacKinnon R (2003b) The principle of gating charge  
movement in a voltage-dependent K<sup>+</sup> channel. *Nature* **423**(6935):42-48.
- Kass RS, Arena JP and Chin S (1991) Block of L-type calcium channels by charged  
dihydropyridines. Sensitivity to side of application and calcium. *J Gen Physiol* **98**(1):63-  
75.
- Kurokawa J, Adachi-Akahane S and Nagao T (1997) 1,5-Benzothiazepine binding domain is  
located on the extracellular side of the cardiac L-type Ca<sup>2+</sup> channel. *Mol Pharmacol*  
**51**:262-268.
- Kwan YW, Bangalore R, Lakitsh M, Glossmann H and Kass RS (1995) Inhibition of cardiac L-  
type calcium channels by quaternary amlodipine: implications for pharmacokinetics and  
access to dihydropyridine binding site. *J Mol Cell Cardiol* **27**(1):253-262.
- Lazaridis T and Karplus M (1999) Discrimination of the native from misfolded protein models  
with an energy function including implicit solvation. *J Mol Biol* **288**(3):477-487.

- Lee PJ, Sunami A and Fozzard HA (2001) Cardiac-specific external paths for lidocaine, defined by isoform-specific residues, accelerate recovery from use-dependent block. *Circ Res* **89**(11):1014-1021.
- Lenaeus MJ and Gross A (2008) Structural basis of quaternary ammonium binding to potassium channels. *Bipohys J S-2008*:943-Plat.
- Li HL, Galue A, Meadows L and Ragsdale DS (1999) A molecular basis for the different local anesthetic affinities of resting versus open and inactivated states of the sodium channel. *Mol Pharmacol* **55**(1):134-141.
- Li Z and Scheraga HA (1987) Monte Carlo-minimization approach to the multiple-minima problem in protein folding. *Proc Natl Acad Sci U S A* **84**(19):6611-6615.
- Lipkind GM and Fozzard HA (2000) KcsA crystal structure as framework for a molecular model of the Na(+) channel pore. *Biochemistry* **39**(28):8161-8170.
- Lipkind GM and Fozzard HA (2005) Molecular modeling of local anesthetic drug binding by voltage-gated sodium channels. *Mol Pharmacol* **68**(6):1611-1622.
- Long SB, Campbell EB and Mackinnon R (2005a) Crystal structure of a mammalian voltage-dependent Shaker family K<sup>+</sup> channel. *Science* **309**(5736):897-903.
- Long SB, Campbell EB and Mackinnon R (2005b) Voltage sensor of Kv1.2: structural basis of electromechanical coupling. *Science* **309**(5736):903-908.
- McNulty MM, Edgerton GB, Shah RD, Hanck DA, Fozzard HA and Lipkind GM (2007) Charge at the lidocaine binding site residue Phe-1759 affects permeation in human cardiac voltage-gated sodium channels. *J Physiol* **581**(Pt 2):741-755.
- Nau C and Wang GK (2004) Interactions of local anesthetics with voltage-gated Na<sup>+</sup> channels. *J Membr Biol* **201**(1):1-8.

- Nau C, Wang SY and Wang GK (2003) Point mutations at L1280 in Nav1.4 channel D3-S6 modulate binding affinity and stereoselectivity of bupivacaine enantiomers. *Mol Pharmacol* **63**(6):1398-1406.
- Nettleton J and Wang GK (1990) pH-dependent binding of local anesthetics in single batrachotoxin-activated Na<sup>+</sup> channels. Cocaine vs. quaternary compounds. *Biophys J* **58**(1):95-106.
- O'Leary ME and Chahine M (2002) Cocaine binds to a common site on open and inactivated human heart (Na<sup>v</sup>)1.5 sodium channels. *J Physiol* **541**(Pt 3):701-716.
- O'Leary ME, Digregorio M and Chahine M (2003) Closing and inactivation potentiate the cocaethylene inhibition of cardiac sodium channels by distinct mechanisms. *Mol Pharmacol* **64**(6):1575-1585.
- Qu Y, Rogers J, Tanada T, Scheuer T and Catterall WA (1995) Molecular determinants of drug access to the receptor site for antiarrhythmic drugs in the cardiac Na<sup>+</sup> channel. *Proc Natl Acad Sci U S A* **92**(25):11839-11843.
- Ragsdale DS, McPhee JC, Scheuer T and Catterall WA (1994) Molecular determinants of state-dependent block of Na<sup>+</sup> channels by local anesthetics. *Science* **265**(5179):1724-1728.
- Ruetsch YA, Boni T and Borgeat A (2001) From cocaine to ropivacaine: the history of local anesthetic drugs. *Curr Topics Med Chem* **1**(3):175-182.
- Santarelli VP, Eastwood AL, Dougherty DA, Ahern CA and Horn R (2007a) Calcium block of single sodium channels: role of a pore-lining aromatic residue. *Biophys J* **93**(7):2341-2349.
- Santarelli VP, Eastwood AL, Dougherty DA, Horn R and Ahern CA (2007b) A cation-pi interaction discriminates among sodium channels that are either sensitive or resistant to tetrodotoxin block. *J Biol Chem* **282**(11):8044-8051.

- Sasaki K, Makita N, Sunami A, Sakurada H, Shirai N, Yokoi H, Kimura A, Tohse N, Hiraoka M and Kitabatake A (2004) Unexpected mexiletine responses of a mutant cardiac Na<sup>+</sup> channel implicate the selectivity filter as a structural determinant of antiarrhythmic drug access. *Mol Pharmacol* **66**(2):330-336.
- Sato C, Ueno Y, Asai K, Takahashi K, Sato M, Engel A and Fujiyoshi Y (2001) The voltage-sensitive sodium channel is a bell-shaped molecule with several cavities. *Nature* **409**(6823):1047-1051.
- Scheib H, McLay I, Guex N, Clare JJ, Blaney FE, Dale TJ, Tate SN and Robertson GM (2006) Modeling the pore structure of voltage-gated sodium channels in closed, open, and fast-inactivated conformation reveals details of site 1 toxin and local anesthetic binding. *J Mol Model* **12**(6):813-822.
- Seydl K, Kimball D, Schindler H and Romanin C (1993) The benzazepine/benzothiazepine binding domain of the cardiac L-type Ca<sup>2+</sup> channel is accessible only from the extracellular side. *Pflugers Arch* **424**:552-554.
- Singh J and Thornton JM (1985) The Interaction between Phenylalanine Rings in Proteins. *FEBS letters* **191**(1):1-6.
- Starmer CF, Grant AO and Strauss HC (1984) Mechanisms of use-dependent block of sodium channels in excitable membranes by local anesthetics. *Biophysical journal* **46**(1):15-27.
- Struyk AF and Cannon SC (2002) Slow inactivation does not block the aqueous accessibility to the outer pore of voltage-gated Na channels. *J Gen Physiol* **120**:509-516.
- Sunami A, Dudley SC, Jr. and Fozzard HA (1997) Sodium channel selectivity filter regulates antiarrhythmic drug binding. *Proc Natl Acad Sci U S A* **94**(25):14126-14131.

- Sunami A, Glaaser IW and Fozzard HA (2000) A critical residue for isoform difference in tetrodotoxin affinity is a molecular determinant of the external access path for local anesthetics in the cardiac sodium channel. *Proc Natl Acad Sci U S A* **97**(5):2326-2331.
- Sunami A, Glaaser IW and Fozzard HA (2001) Structural and gating changes of the sodium channel induced by mutation of a residue in the upper third of IVS6, creating an external access path for local anesthetics. *Mol Pharmacol* **59**(4):684-691.
- Terlau H, Heinemann SH, Stuhmer W, Pusch M, Conti F, Imoto K and Numa S (1991) Mapping the site of block by tetrodotoxin and saxitoxin of sodium channel II. *FEBS letters* **293**(1-2):93-96.
- Tikhonov DB, Bruhova I and Zhorov BS (2006) Atomic determinants of state-dependent block of sodium channels by charged local anesthetics and benzocaine. *FEBS Lett* **580**(26):6027-6032.
- Tikhonov DB, Mellor IR and Usherwood PN (2004) Modeling noncompetitive antagonism of a nicotinic acetylcholine receptor. *Biophys J* **87**(1):159-170.
- Tikhonov DB and Zhorov BS (1998) Kinked-helices model of the nicotinic acetylcholine receptor ion channel and its complexes with blockers: simulation by the Monte Carlo minimization method. *Biophys J* **74**(1):242-255.
- Tikhonov DB and Zhorov BS (2005a) Modeling P-loops domain of sodium channel: homology with potassium channels and interaction with ligands. *Biophys J* **88**(1):184-197.
- Tikhonov DB and Zhorov BS (2005b) Sodium channel activators: model of binding inside the pore and a possible mechanism of action. *FEBS Lett* **579**(20):4207-4212.
- Tikhonov DB and Zhorov BS (2007) Sodium Channels: Ionic Model of Slow Inactivation and State-Dependent Drug Binding. *Biophys J* **93**(3):1557-1570.



- Wang GK, Quan C and Wang S (1998) A common local anesthetic receptor for benzocaine and etidocaine in voltage-gated mu1 Na<sup>+</sup> channels. *Pflugers Arch* **435**(2):293-302.
- Wang SY, Mitchell J, Tikhonov DB, Zhorov BS and Wang GK (2006) How batrachotoxin modifies the sodium channel permeation pathway: computer modeling and site-directed mutagenesis. *Mol Pharmacol* **69**(3):788-795.
- Wang SY, Tikhonov DB, Zhorov BS, Mitchell J and Wang GK (2007a) Irreversible block of cardiac mutant Na<sup>+</sup> channels by batrachotoxin. *Channels* **1**:178-188.
- Wang SY, Tikhonov DB, Zhorov BS, Mitchell J and Wang GK (2007b) Serine-401 as a batrachotoxin- and local anesthetic-sensing residue in the human cardiac Na<sup>+</sup> channel. *Pflugers Arch* **454**(2):277-287.
- Weiner SJ, Kollman PA, Case DA, Singh UC, Chio C, Alagona G, Profeta S and Weiner PK (1984) A new force field for molecular mechanical simulation of nucleic acids and proteins. *J Am Chem Soc* **106**:765-784.
- Weiner SJ, Kollman PA, Nguyen DT and Case DA (1986) An All Atom Force-Field for Simulations of Proteins and Nucleic-Acids. *J Comput Chem* **7**(2):230-252.
- Wright SN, Wang SY, Kallen RG and Wang GK (1997) Differences in steady-state inactivation between Na channel isoforms affect local anesthetic binding affinity. *Biophys J* **73**(2):779-788.
- Wright SN, Wang SY and Wang GK (1998) Lysine point mutations in Na<sup>+</sup> channel D4-S6 reduce inactivated channel block by local anesthetics. *Mol Pharmacol* **54**(4):733-739.
- Xu YQ, Crumb WJ, Jr. and Clarkson CW (1994) Cocaethylene, a metabolite of cocaine and ethanol, is a potent blocker of cardiac sodium channels. *J Pharmacol Exp Ther* **271**(1):319-325.

- Yamagishi T, Janecki M, Marban E and Tomaselli GF (1997) Topology of the P segments in the sodium channel pore revealed by cysteine mutagenesis. *Biophys J* **73**(1):195-204.
- Yamaguchi S, Zhorov BS, Yoshioka K, Nagao T, Ichijo H and Adachi-Akahane S (2003) Key roles of Phe1112 and Ser1115 in the pore-forming IIS5-S6 linker of L-type Ca<sup>2+</sup> channel alpha1C subunit (CaV 1.2) in binding of dihydropyridines and action of Ca<sup>2+</sup> channel agonists. *Mol Pharmacol* **64**(2):235-248.
- Yarov-Yarovoy V, Brown J, Sharp EM, Clare JJ, Scheuer T and Catterall WA (2001) Molecular determinants of voltage-dependent gating and binding of pore-blocking drugs in transmembrane segment IIS6 of the Na(+) channel alpha subunit. *J Biol Chem* **276**(1):20-27.
- Yarov-Yarovoy V, McPhee JC, Idsvoog D, Pate C, Scheuer T and Catterall WA (2002) Role of amino acid residues in transmembrane segments IS6 and IIS6 of the Na<sup>+</sup> channel alpha subunit in voltage-dependent gating and drug block. *J Biol Chem* **277**(38):35393-35401.
- Zhorov BS and Tikhonov DB (2004) Potassium, sodium, calcium and glutamate-gated channels: pore architecture and ligand action. *J Neurochem* **88**(4):782-799.
- Zhou M, Morais-Cabral JH, Mann S and MacKinnon R (2001) Potassium channel receptor site for the inactivation gate and quaternary amine inhibitors. *Nature* **411**(6838):657-661.
- Zhou Y and MacKinnon R (2003) The occupancy of ions in the K<sup>+</sup> selectivity filter: charge balance and coupling of ion binding to a protein conformational change underlie high conduction rates. *Journal of molecular biology* **333**(5):965-975.

## FOOTNOTES

This study was supported by the grant to BSZ from the Canadian Institutes of Health Research (CIHR). IB is a recipient of the CIHR Canada Graduate Scholarships Doctoral Award. Computations were performed using the facilities of the Shared Hierarchical Academic Research Computing Network (SHARCNET: [www.sharcnet.ca](http://www.sharcnet.ca)).

## Figure Legends

**Figure 1.** Chemical structures of LAs that are used in calculations.

**Figure 2.** Searching for energetically favorable binding modes of QX-314 in the closed Na<sub>v</sub>1.5 with a water molecule in the selectivity filter. The inner helices and P-loops of domains I, II, III, and IV are colored cyan, orange, green, and violet, respectively. The outer helices are shown as gray strands. The water molecule is space-filled. The side chains of residues in the DEKA locus as well as conserved F<sup>4i15</sup> and Y<sup>4i22</sup> are shown as sticks. The ligand is wire-frame with the ammonium nitrogen shown as a blue sphere. **A** and **B**, Side and top views at the superposition of starting points. For clarity, only 6,000 of the 60,000 starting points are shown. **C**, Fifty lowest-energy binding modes. **D**, **E**, and **F**, Superposition of the lowest energy vertical, angular, and horizontal binding modes, respectively. For clarity the outer helices are not shown in **C-F**.

**Figure 3.** Searching for energetically favorable binding modes of cocaine in the closed Na<sub>v</sub>1.5 with a water molecule (**A**, **C**, **E**) or Na<sup>+</sup> ion (**B**, **D**, **F**) in the DEKA locus. For clarity the outer helices are not shown. **A** and **B**, Fifty lowest-energy binding modes in the H<sub>2</sub>O-DEKA and Na<sup>+</sup>-DEKA models, respectively. **C**, A vertical binding mode of cocaine. The ligand's aromatic

group interacts with three aromatic residues in positions *i22*. **D**, The energetically most favorable binding mode of cocaine in the Na<sup>+</sup>-DEKA model. The oxygen atoms of cocaine approach the Na<sup>+</sup> ion, while the aromatic ring of the drug extends to the sidewalk between helices IIIS6 and IVS6. **E** and **F**, The superposition of the energetically best horizontal binding modes.

**Figure 4.** Searching for energetically favorable binding modes of tetracaine in the closed Na<sub>v</sub>1.5 channel with a water molecule in the DEKA locus. **A**, Fifty lowest-energy complexes. In most of the complexes, the drug's aromatic ring protrudes in the III/IV domain interface. **B**, The superposition of three lowest-energy complexes representing the horizontal binding mode. **C** and **D**, The side and top views of the lowest-energy complex representing the horizontal binding mode. Note  $\pi$ -stacking of the drug's aromatic ring with F<sup>4i15</sup>.

**Figure 5.** Exploring hypothetical access pathways of QX-314. **A** and **B**, Superposition of the MC-minimized structures obtained for QX-314 pulled out of the pore through the selectivity filter (**A**) and the closed activation gate (**B**). QX-314, DEKA residues, F<sup>4i15</sup> and Y<sup>4i22</sup> are shown as sticks. For clarity, domain I is not shown. **C**, The MC-minimized energy profiles showing the total drug-channel energy and its components. From the starting position 0, which corresponds to the lowest-energy vertical binding mode of QX-314 (Fig. 2D), the ligand was pulled at 0.5 Å steps either through the selectivity filter (positions 0 to 25) or through the activation gate (positions 0 to -25).

**Figure 6.** Pulling QX-314 through the sidewalk, between segments IIIP, IIIS6, and IVS6. **A** and **B**, The side and top views of the superposition of QX-314 pulled from the starting position 0, which corresponds to the horizontal binding found from random sampling (Fig. 2 F).

**Figure 7.** The MC-minimized energy profile of QX-314 pulled through the sidewalk. **A**, The energy profile with total drug-channel energy and its components. Position 0 corresponds to the lowest-energy drug-channel complex, which was found in the multi-MCM search and which

represents the horizontal binding mode (Fig. 2 *F*). The ligand was pulled at 0.5 Å steps. **B**, The energy profile of QX-314 pulled through the III-IV interface of the H<sub>2</sub>O-DEKA and Na<sup>+</sup>-DEKA models. **C** and **D**, Most significant energy contributors to the energy profile.

**Figure 8.** A scheme of coupled movement of Na<sup>+</sup> and a LA molecule in the closed Na<sup>+</sup> channel. **A**, An LA molecule accessing the inner pore via the sidewalk repels the resident Na<sup>+</sup> ion, which can move away via the unblocked outer pore and release the nucleophilic central cavity for binding of the LA ammonium group. **B**, When the outer pore is blocked by TTX, the Na<sup>+</sup> ion in the central cavity lacks a hydrophilic escape route, remains in the central cavity, and prevents the LAs access. **C**, the μ-CTX mutant (green ribbon), binds in the outer pore, but does not completely block the Na<sup>+</sup> current. The Na<sup>+</sup> ion can escape through the incompletely blocked outer pore and free the nucleophilic central cavity for the LAs binding. See *Discussion* for more details.

**TABLES**

**Table 1.** Sequences of ion channels <sup>a,b</sup> and effect of mutations in Na<sup>+</sup> channels <sup>c-1</sup>

Channel	Segment <sup>b</sup>	#	1	11	21			
KcsA	M1	o	14	ALHWRAAGAA	TVLLVIVLLA	GSYLAVLAER		
Na <sub>v</sub> 1.5	IS5	1o	242	IQSVKKLADV	MVLTVFCLSV	FALIGLQLFM		
	IIS5	2o	825	GNSVGALGNL	TLVLAIIVFI	FAVVGMQLFG		
	IIIS5	3o	1321	VGAI PSIMNV	LLVCLIFWLI	FSIMGVNLFA		
	IVS5	4o	1644	MMSLPALFNI	GLLLFLVMFI	YSIFGMANFA		
			<b>33</b>	<b>41</b>	<b>51</b>			
KcsA	P	p	59	LITYPRAL	WWSVETATTV	GYGDLYPV		
Na <sub>v</sub> 1.4	IP	1p	383	YDTFSWAF	LALFRLMTQD	<u>Y</u> WENLFQL	c	
	IIP	2p	738	MNDFHHSF	LIVFRILCGE	WIETMWDC	c	
	IIIP	3p	1220	YDNVGLGY	LSSLQVATFK	GWMDIMYA		
Na <sub>v</sub> 1.5	IVP	4p	1512	FETFGENSI	ICLFEITTS <u>A</u>	GWDGLLNP	c	
	IP	1p	356	FDSFAWAF	LALFRLMTQD	<u>C</u> WERLYQQ	d	
	IIP	2p	884	MMDFHAF	LIIFRILCGE	WIETMWDC		
	IIIP	3p	1404	FDNVGAGY	LALLQVATFK	GWMDIMYA		
	IVP	4p	1696	FQTFANSM	LCLFQITTS <u>A</u>	GWDGLLSP	e	
Pore-facing position					**	***		
Sidewalk-facing position in IIIP					*	***		
			<b>1</b>	<b>11</b>	<b>21</b>	<b>31</b>		
KcsA	M2	i	86	LWGRLVAVVV	MVAGITSFGL	VTAALATWFV	GREQ	
Na <sub>v</sub> 1.2	IS6	1i	399	KTYMIFVVLV	I FLGSFYLIN	LILAVVAMAY	EEQN	f
	IIS6	2i	957	TMCLTVFMMV	<u>M</u> VIGNLVVLN	LFLALLLSSF	SSDN	g
	IIIS6	3i	1447	LYMYLYFVIF	IIFGSFFTLN	LFI <u>G</u> VIIDNF	NQQK	h
	IVS6	4i	1750	SVGIFFFVSY	<u>I</u> IISFLVVVN	MYIAVILENF	SVAT	i
Na <sub>v</sub> 1.4	IS6	1i	415	KTYMIFVVI	I FLGSFYLIN	LILAVVAMAY	AEQN	
	IIS6	2i	770	AMCLTVFLMV	MVIGNLVVLN	LFLALLLSSF	SADS	
	IIIS6	3i	1262	LYMYLYFVIF	IIFGSFFTLN	LFI <u>G</u> VIIDNF	NQQK	j
	IVS6	4i	1565	SIGICFF <u>C</u> SY	<u>I</u> IISFLIVVN	MYIAIILENF	NVAT	k
Na <sub>v</sub> 1.5	IS6	1i	388	KIYMIFVMLV	I FLGSFYLVN	LILAVVAMAY	EEQN	
	IIS6	2i	916	SLCLLVFLLV	MVIGNLVVLN	LFLALLLSSF	SADN	
	IIIS6	3i	1446	LYMYIYFVVF	IIFGSFFTLN	LFI <u>G</u> VIIDNF	NQQK	
	IVS6	4i	1748	AVGILFF <u>T</u> TY	<u>I</u> IISFLIVVN	MYIAIILENF	SVAT	l
Pore-facing position					*	*	**	*
Sidewalk-facing positions IIIS6						*	*	
Sidewalk-facing positions IVS6					*	**	*	

<sup>a</sup> Bold-typed are residues whose mutations are described under footnotes referred to in the rightmost column. Residues whose mutations affect closed-channel block are shaded. Residues whose mutations affect access of LAs are underlined.

- <sup>b</sup> The standard segment name includes the domain number and symbols S5, S6, or P, for respective transmembrane segment or membrane-reentering P-loop. An alternative segment name, which is used in residue labels, includes the domain number and symbols o, p, and i for the outer helices, inner helices, and P-loops, respectively. The absolute numbers (#) of the first residue in a segment are shown for the following sequences: Na<sub>v</sub>1.2 (SCN2A\_RAT), Na<sub>v</sub>1.4 (SCN4A\_RAT), and Na<sub>v</sub>1.5 (SCN5A\_RAT). Relative numbers of residues are shown above the aligned sequences. For the transmembrane segments, the relative numbers are counted from the beginnings of the respective KcsA helices as seen in the X-ray structure (Doyle et al., 1998). Relative numbers of residues in P-loop are counted from the DEKA-locus, whose residues are assigned number 50 to avoid negative numbers for residues in P-helices.
- <sup>c</sup> Mutations at the DEKA locus (D<sup>1p50</sup>A, E<sup>2p50</sup>A, and A<sup>4p50</sup>D) allowed external block by QX-222 and QX-314 and accelerated the recovery from block by internal QX-314 (Sunami et al., 1997). Mutation Y<sup>1p51</sup>C enabled the external block by QX-222 (Sunami et al., 2000).
- <sup>d</sup> Mutation C<sup>1p51</sup>Y reduced the external QX-314 block (Sunami et al., 2000).
- <sup>e</sup> Mutation S<sup>4p49</sup>L accelerated recovery of hNa<sub>v</sub>1.5 from internally applied QX-314 and enhanced tonic block by mexiletine and QX-314 (Sasaki et al., 2004).
- <sup>f</sup> Mutation Y<sup>1i17</sup>A increased the affinity of etidocaine to the closed channel (Yarov-Yarovoy et al., 2002).
- <sup>g</sup> Mutations M<sup>2i11</sup>A, N<sup>2i15</sup>A, and V<sup>2i18</sup>A increased closed-channel block by etidocaine (Yarov-Yarovoy et al., 2002).
- <sup>h</sup> Mutations L<sup>3i19</sup>A, N<sup>3i20</sup>A, and I<sup>3i23</sup>A decreased affinity of inactivated channels to LAs, but did not decrease the closed-channel block (Yarov-Yarovoy et al., 2001). Mutations L<sup>3i19</sup>A and N<sup>3i20</sup>A increased the closed-channel block by lamotrigine and etidocaine. Mutation I<sup>3i23</sup>A increased the affinity for lamotrigine but not etidocaine to the closed channel.

- <sup>i</sup> Mutation I<sup>4i11</sup>A accelerated the channel recovery after use-dependent block and allowed external QX-314 block (Ragsdale et al., 1994). Alanine mutations of F<sup>4i15</sup>, N<sup>4i20</sup>, and Y<sup>4i22</sup> significantly decreased use-dependent block by etidocaine (Ragsdale et al., 1994). In the Na<sub>v</sub>1.3 channel, closed-channel block requires a hydrophobic residue at position *4i15*, while use-dependent block by tetracaine requires an aromatic residue *4i15* and Y<sup>4i22</sup> (Li et al., 1999).
- <sup>j</sup> Mutation of L<sup>3i19</sup> had no effect on closed-channel block by bupivacaine (Nau et al., 2003).
- <sup>k</sup> Mutation C<sup>4i8</sup>T allowed the external QX-222 block (Sunami et al., 2000). Mutant I<sup>4i11</sup>A allows block by the external QX-314 (Wang et al., 1998) and QX-222 (Sunami et al., 2001). Benzocaine and etidocaine are less potent in the F<sup>4i15</sup>A mutant (Wang et al., 1998). Lysine substitutions showed that Y<sup>4i22</sup> is important for the use-dependent block, but not the closed-channel block by cocaine, while F<sup>4i15</sup> and N<sup>4i20</sup> are important for both the use-dependent and closed-channel block (Wright et al., 1998).
- <sup>l</sup> T<sup>4i8</sup>V reduced external QX-314 block; F<sup>4i15</sup>A inhibited the binding of both external and internal QX-314 (Qu et al., 1995). I<sup>4i11</sup>C accelerated recovery and facilitated closed-state untrapping of cocaethanol (O'Leary et al., 2003). Mutation Y<sup>4i22</sup>C significantly reduced use-dependent block by cocaine (O'Leary and Chahine, 2002).



**Table 2.** Energetically favorable binding modes of LAs in the closed Na<sub>v</sub>1.5 with the DEKA locus loaded by either H<sub>2</sub>O or Na<sup>+</sup>.

Ligand-channel energy and its components <sup>a</sup>	Cocaine <sup>b</sup>			QX-314 <sup>b</sup>			Tetracaine
	Vertical <sup>c</sup>		Horizontal	Vertical <sup>c</sup>		Horizontal	Horizontal <sup>d</sup>
	H <sub>2</sub> O	H <sub>2</sub> O	Na <sup>+</sup>	H <sub>2</sub> O	H <sub>2</sub> O	Na <sup>+</sup>	H <sub>2</sub> O
Total	-40.6	-38.2	-36.2	-39.3	-39.0	-31.3	-35.2
van der Waals	-24.4	-26.1	-31.5	-23.3	-21.9	-22.7	-27.1
Desolvation	13.2	23.3	28.1	8.7	14.1	14.2	14.4
Electrostatics	-29.4	-35.5	-32.8	-24.8	-30.8	-22.7	-22.4
Segments <sup>e</sup>							
P-loops	-19.9	-23.3	-30.7	-18.8	-24.6	-25.0	-20.7
All S6s	-19.8	-14.9	-10.8	-19.7	-13.6	-14.1	-12.3
Key determinants of action <sup>f</sup>							
Phe <sup>4i15</sup>	-0.2	-3.9	-2.9	-1.0	-2.2	-2.4	-2.1
Tyr <sup>4i22</sup>	-3.2	-0.6	-0.4	-3.5	-0.4	-0.6	0.0

<sup>a</sup> Ligand-receptor energy, its components, and contributions (kcal/mol) from individual segment and specific residues.

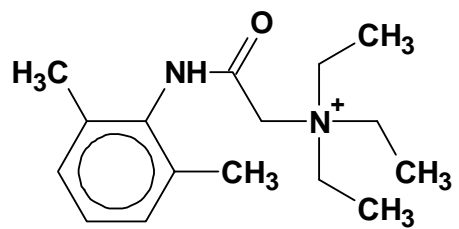
<sup>b</sup> The lowest-energy structure for each binding mode is shown. The entropy contributions were not taken into account, which is a standard approximation in homology modeling. These contributions would partially compensate the large enthalpy of ligand-channel interactions.

<sup>c</sup> The Na<sup>+</sup>-DEKA model energy is not shown because it is much weaker than in the H<sub>2</sub>O-DEKA model.

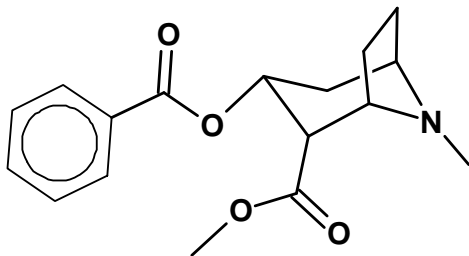
<sup>d</sup> The Na<sup>+</sup>-DEKA model with tetracaine was not explored.

<sup>e</sup> The energy values include both the side chain and backbone contribution to ligand binding.

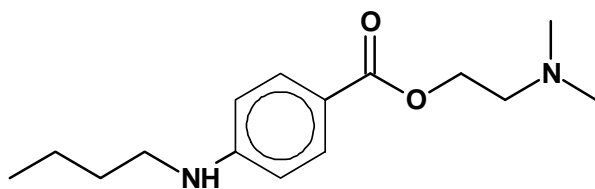
<sup>f</sup> The energy values include only the side chain contributions to ligand binding.



QX-314



Cocaine



Tetracaine

Fig. 1

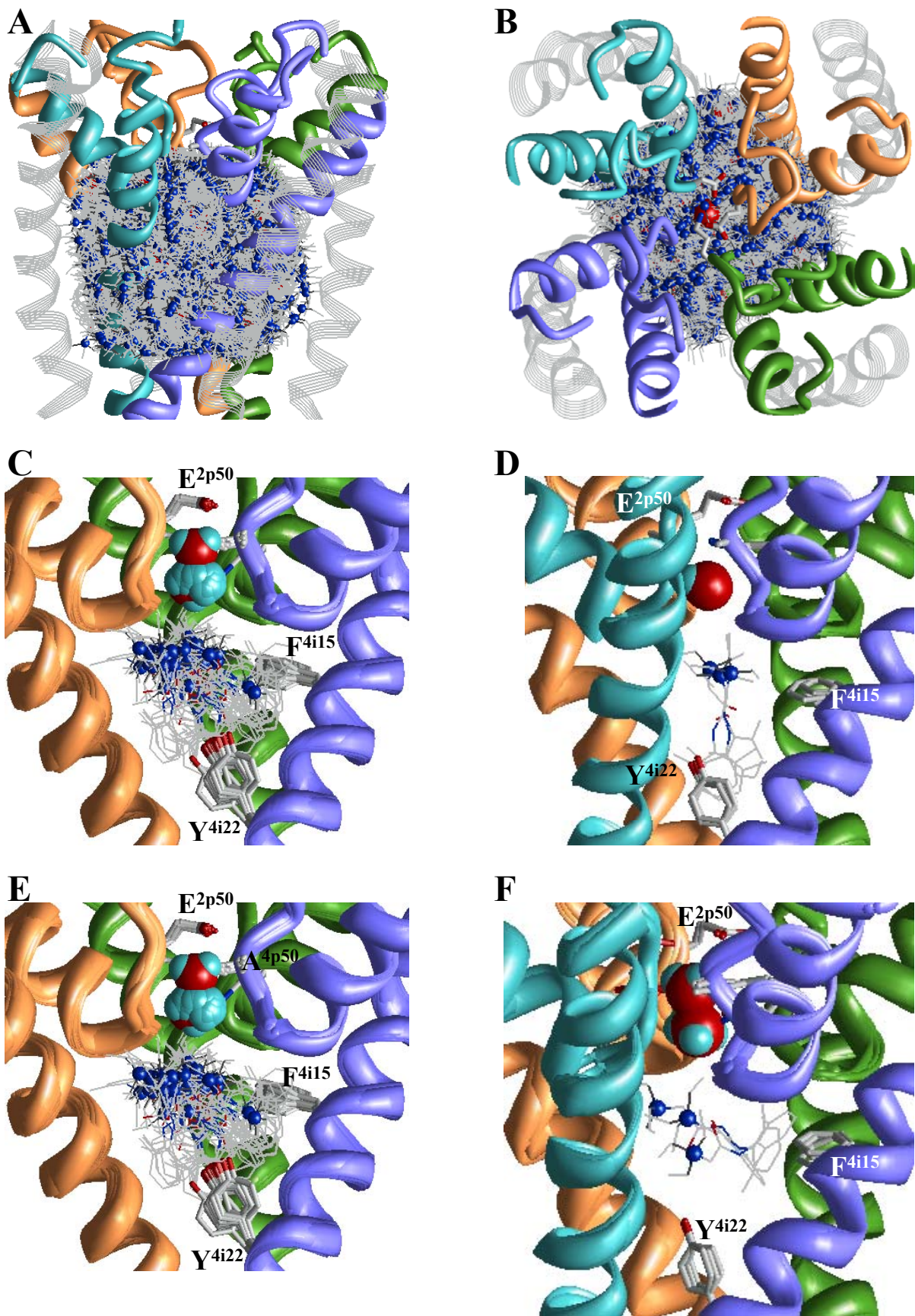


Fig. 2



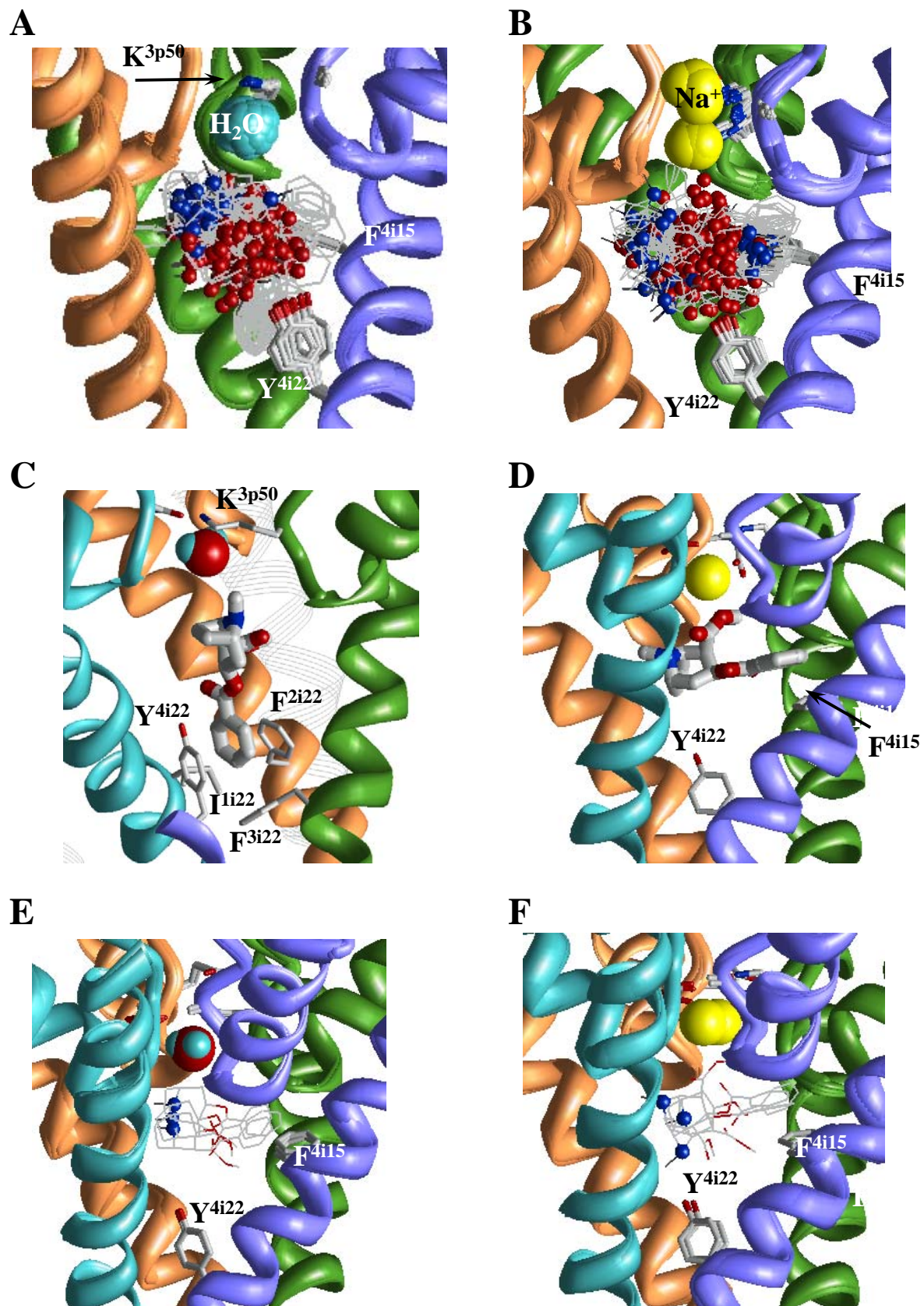


Fig. 3

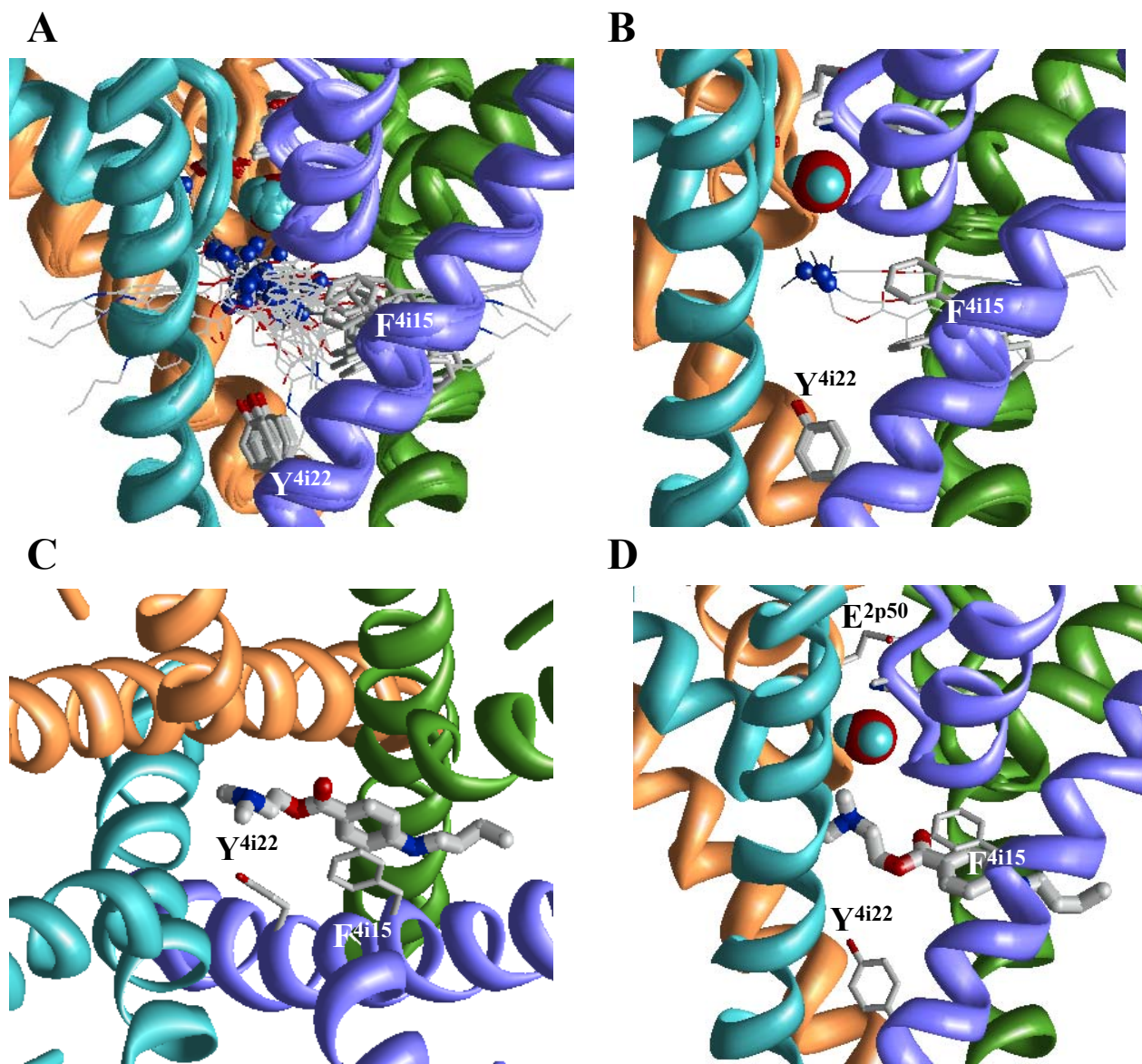


Fig. 4



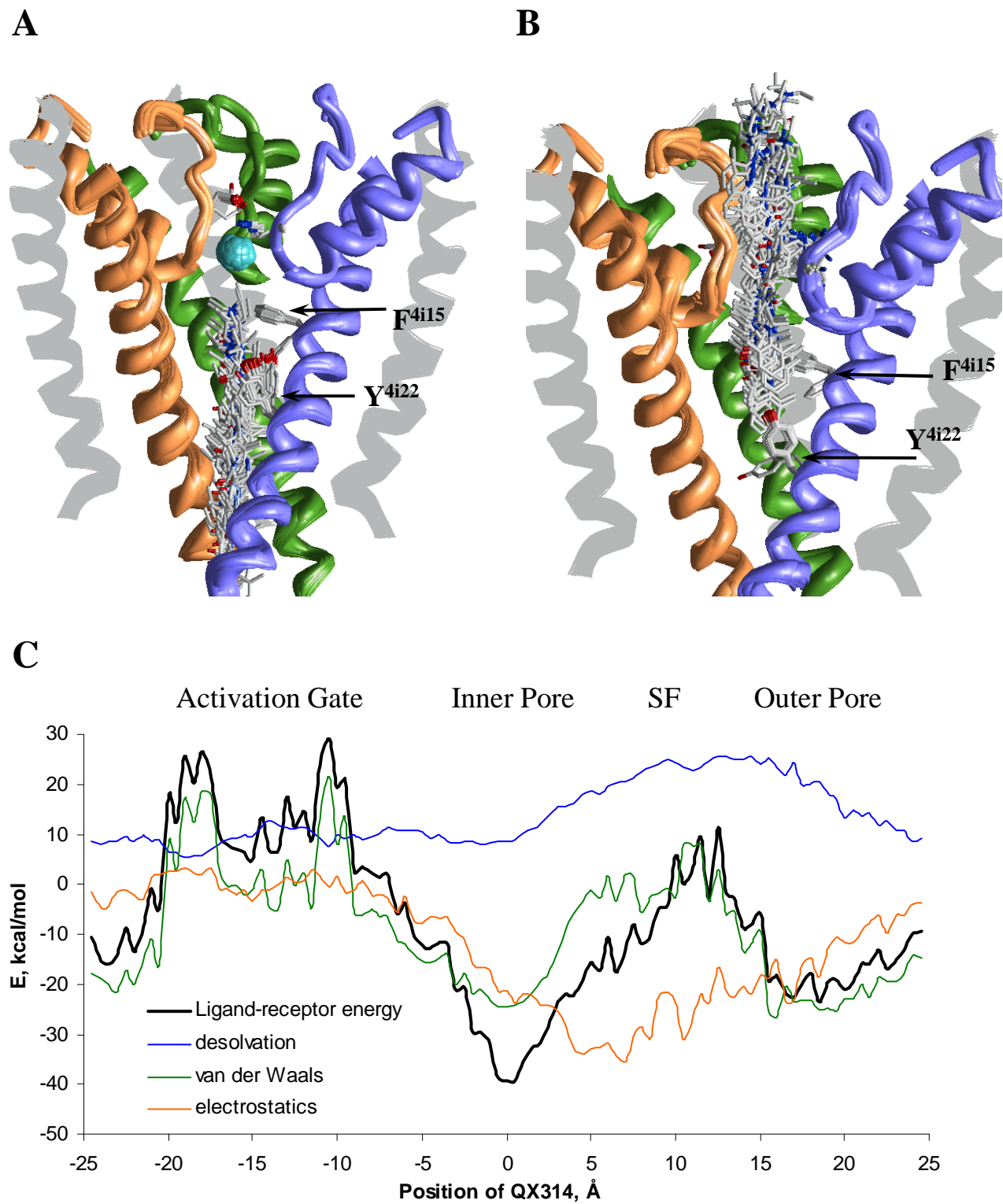


Fig. 5

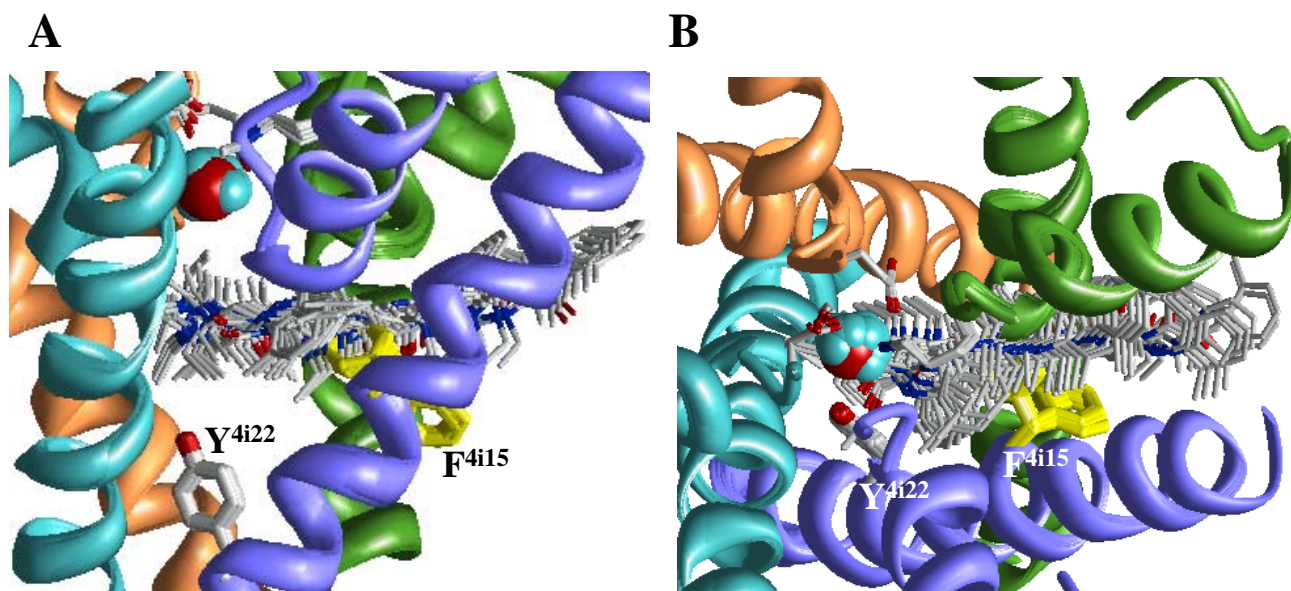


Fig. 6

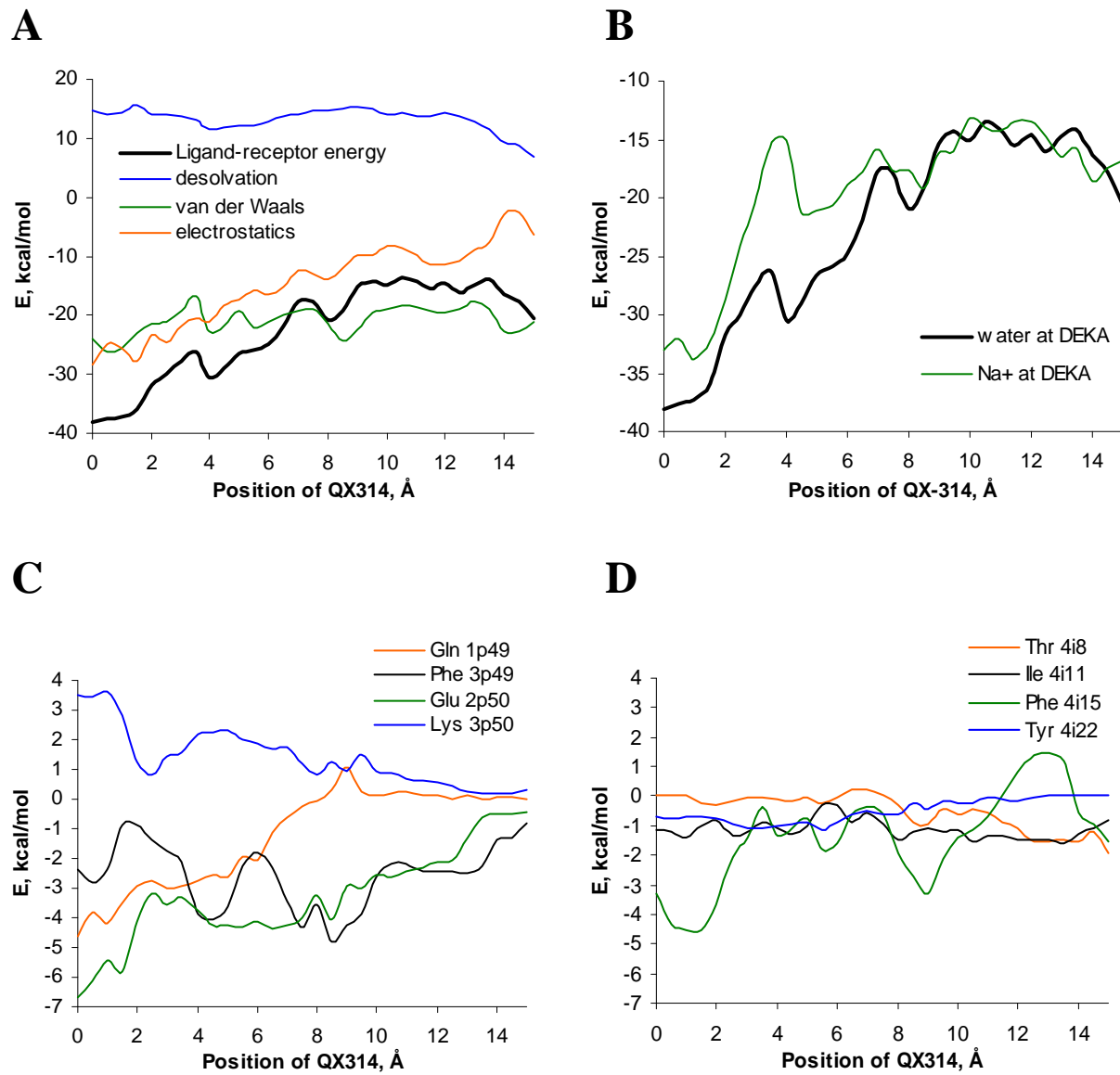


Fig. 7



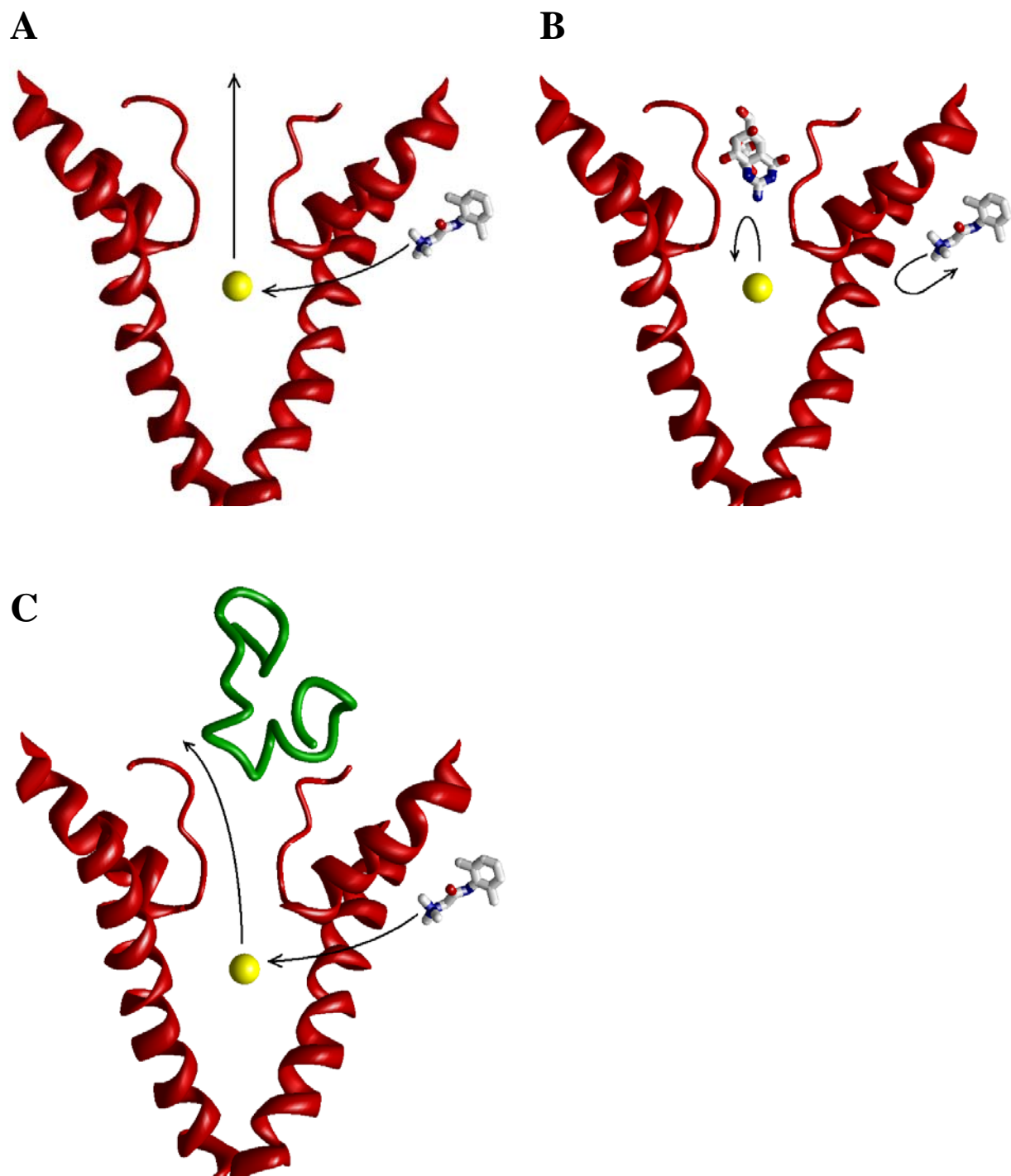


Fig. 8